nature climate change

SUPPLEMENTARY INFORMATION

DOI: 10.1038/NCLIMATE2470

Rising temperatures reduce global wheat production

Supplementary Materials

Rising temperatures reduce global wheat production

S. Asseng, F. Ewert, P. Martre, R.P. Rötter, D.B. Lobell, D. Cammarano, B.A. Kimball, M.J. Ottman, G.W. Wall, J.W. White, M.P. Reynolds, P.D. Alderman, P.V.V. Prasad, P.K. Aggarwal, J. Anothai, B. Basso, C. Biernath, A.J. Challinor, G. De Sanctis, J. Doltra, E. Fereres, M. Garcia-Vila, S. Gayler, G. Hoogenboom, L.A. Hunt, R.C. Izaurralde, M. Jabloun, C.D. Jones, K.C. Kersebaum, A.-K. Koehler, C. Müller, S. Naresh Kumar, C. Nendel, G. O'Leary, J. E. Olesen, T. Palosuo, E. Priesack, E. Eyshi Rezaei, A.C. Ruane, M.A. Semenov, I. Shcherbak, C. Stöckle, P. Stratonovitch, T. Streck, I. Supit, F. Tao, P. Thorburn, K. Waha, E. Wang, D. Wallach, J. Wolf, Z. Zhao, and Y. Zhu

Correspondance to: sasseng@ufl.edu

This PDF file includes:

Supplementary Materials and Methods

Thirty wheat crop models, including 29 deterministic process-based simulation models and one statistical model, (Supplementary Table S1 and S2) were compared within the Agricultural Model Intercomparison and Improvement Project[1] (AgMIP; www.agmip.org), with two data sets from quality-assessed field experiments (sentinel site data).

Hot-Serial-Cereal (HSC)

One site was the Hot-Serial-Cereal (HSC) experiment with time-of-sowing and artificial infrared heating treatments under field conditions using cv Yecora Rojo, characterized by low to no vernalization requirements and photoperiod sensetivity[2, 3]. Individual field replicates were used from[2, 3] for the simulations which were previously not publicly available (therefore called a "blind" analysis).

All experiments were well watered and fertilized with temperature being the most important variable. A model inter-comparison was carried out using standardized protocols and several steps of calibration.

Supplementary Table S1. Crop models (30) used in AgMIP Wheat study.

Model (version)	Reference	Documentation
APSIM-E	4-6	http://www.apsim.info/Wiki/
APSIM-Nwheat (V.1.55)	4, 7, 8	http://www.apsim.info
APSIM-Wheat (V.7.3)	4	http://www.apsim.info/Wiki/
AQUACROP (V.4.0)	9	http://www.fao.org/nr/water/aquacrop.html
CropSyst (V.3.04.08)	10	http://www.bsyse.wsu.edu/CS_Suite/CropSyst/index.html
DAISY (V.5.18)	11, 12	https://code.google.com/p/daisy-model/
DSSAT- CERES (V.4.0.1.0)	13-15	http://www.icasa.net/dssat/
DSSAT-CROPSIM (V4.5.1.013)	14, 16	http://www.icasa.net/dssat/
EPIC (V1102)	17-19	http://epicapex.brc.tamus.edu/
Expert-N (V3.0.10) - CERES (V2.0)	20-23	http://www.helmholtz-muenchen.de/en/iboe/expertn/
Expert-N (V3.0.10) – GECROS (V1.0)	22, 23	http://www.helmholtz-muenchen.de/en/iboe/expertn/

Expert-N (V3.0.10) – SPASS (2.0)	[20, 22-25]	http://www.helmholtz-muenchen.de/en/iboe/expertn/
Expert-N (V3.0.10) - SUCROS (V2)	[20, 22, 23, 26]	http://www.helmholtz-muenchen.de/en/iboe/expertn/
FASSET (V.2.0)	[27, 28]	http://www.fasset.dk
GLAM (V.2)	[29, 30]	http://www.see.leeds.ac.uk/research/icas/climate-impacts-group/research/glam/
HERMES (V.4.26)	[31, 32]	http://www.zalf.de/en/forschung/institute/lsa/forschung/oekomod/hermes
INFOCROP (V.1)	[33]	http://www.iari.res.in
LINTUL (V.1)	[34, 35]	http://models.pps.wur.nl/models
LOBELL	[36]	Request from dlobell@stanford.edu
LPJmL (V3.2)	[37-42]	http://www.pik-potsdam.de/research/projects/lpjweb
MCWLA-Wheat (V.2.0)	[43-46]	Request from taofl@igsnrr.ac.cn
MONICA (V.1.0)	[47]	http://monica.agrosystem-models.com
OLEARY (V.7)	[48-51]	Request from gjoleary@yahoo.com
SALUS (V.1.0)	[52, 53]	http://www.salusmodel.net
SIMPLACE (V.1)	[54]	Request from frank.ewert@uni-bonn.de
SIRIUS (V2010)	[55-58]	http://www.rothamsted.ac.uk/mas-models/sirius.php
SiriusQuality (V.2.0)	[59-61]	http://www1.clermont.inra.fr/siriusquality/
STICS (V.1.1)	[62, 63]	http://www.avignon.inra.fr/agroclim_stics_eng/
WHEATGROW	[64-70]	Request from yanzhu@njau.edu.cn
WOFOST (V.7.1)	[71]	http://www.wofost.wur.nl

Supplementary Table S2. Consideration of temperature in wheat simulation models (For details see Alderman et al.[72]).

Model	**Phenology**	**Vernalization**	**Light Utilization**	**Respiration**	**Leaf growth**	**Canopy temperature**	**Senescence**	**Grain set**	**Grain growth**	**Grain N Uptake**	**Root growth**	**Cold Hardening**
APSIM-E	Am	Am	Am	-	Am	-	An, Sm	-	Am	Am	Am	-
APSIM-Nwheat	Am	Am	Am	-	Am	-	Am, Ae, Af	Am	Am	Am	Sm	-
APSIM-wheat	Am	Am, Ax, An	Am	-	Am	-	Am, Af	Am	Am	Am	Sm	-
AQUACROP	Am	-	-	-	Am[1]	-	Am	Ax, An	Am	-	Am	-
CropSyst	Am	Am	Am	-	-	Cm	Am, Ae, Af	Ah	-	-	-	Ah
DAISY	Sm, Am	Am	Am	Am	Am	-	-	Am	Am	Am	Sm	-
DSSAT-CERES	Am	Am	Am	-	Am	-	Am	Am	Am	Am	Am	-
DSSAT-CROPSIM	Am	Am	Am	-	Am	-	Am	Am	Am	Am	Sm	-
EPIC	Am	-	Am	Am	Am	-	Am, An	-	Am	Am	Sm	-
Expert-N – CERES	Cm, Ae, Af	Ax, Cm, An	Ax, An	-	Am	Ax, An	-	-	Ax, Am, An	Ax, Am, An	Cm	-
Expert-N – GECROS	Cx, Cn	Ax, An	Cx, Cn	Am	-	Ax, An	-	-	-	-	-	-
Expert-N – SPASS	Ax, An	Ax, An	Ax, An	Am	-	-	Am	-	-	Am	Sm	-
Expert-N – SUCROS	Ax, An	-	Ax, An	Am	-	-	Am	-	-	-	Ax, An	-
FASSET	Am	Am	Am	-	Am	-	Am	Am	Am	Am	Sm	
GLAM	Am	-	-	-	-	-	Ax	Am	-	-	-	-
HERMES	Am	Am	Am	Am	-	-	Am	-	Am	-	Am	-
INFOCROP	Ah[2]	-	Am	-	Ah[3]	-	Am, Af	Ax, An	Am[4]	Am[4]	-	-
LINTUL	Am	-	Am, An	-	-	-	Am	-	-	-	-	-
LOBELL	-	-	-	-	-	-	-	-	-	-	-	-
LPJmL	Am	Am	Am	Am, Sm	Am	Am	Am	-[5]	-[5]	-	Am[6]	-
MCWLA-Wheat	Am	Am	Am	Am	Am	-	Am, Ae	Am, Ae	Am	-	Am	-

MONICA	Sm, Am	Am	Am	Ax, An	-	-	Am	-	-	-	Am	-
OLEARY	Am	-	Am	-	-		Am	-	Am	-	Am	-
SALUS	Am	Am	Am	-	Am	-	Am, Ae, Af	Am	Am	Am	Sm	-
SIMPLACE	Am	Am	-	-	Am	-	Am	Ax, Ae	-	-	-	-
SIRIUS	Ah, Ch, Sh	Sh	Ah	-	Ah, Ch, Sh	Ah	Ah, Ch	Ch	Ch	Ch	Sh	-
SirusQuality	Sm, Cm	Sm, Cm	Cm	-	Cm	Cm	Cm	Cm	Cm	Cm	Am	-
STICS	Cm	Cm	Cm	-	Cm		Cm, Cf	Cm	Cx, Cn, Ce			-
WHEATGROW	Am	Am	Am	Am	Am	-	Am, Ae	Am	Am	Am	Am	
WOFOST	Am	-	Am	Am	Am	-	Am	-	Am	-	Am	-

Temperature:
A – Air
C – Canopy
S – Soil

Suffix:
m – daily mean
x – daily maximum
n – daily minimum
h – hourly
e – daily extreme maximum (>34 °C)
f – daily frost (<2°C)

[1]Canopy growth; [2]Ah is interpolated from daily minimum and maximum temperatures; [3]for initial growth and later dependent on biomass growth; [4]also biomass dependent; [5]The processes of grain set and growth is not modeled but only the carbon pool for the storage organs which is affected by air temperature; [6]Temperature effects on the equilibrium evapotranspiration rate affect water stress (the ratio between calculations of atmospheric water demand and crop water supply), and thus plant root growth.

CIMMYT data

The second set was the International Heat Stress Genotype Experiment (IHSGE) carried out by CIMMYT that included seven temperature environments, including time-of-sowing treatments[73]. These experimental data were also not publicly available and could therefore be used in a blind test.

The International Heat Stress Genotype Experiment was a 4-year collaboration between CIMMYT and key national agricultural research system partners to identify important physiological traits that have value as predictors of yield at high temperatures [73]. Experimental locations were selected based on a classification of temperature and humidity during the wheat growing cycle. "Hot" and "very hot" locations were defined as having mean temperatures above 17.5 and 22.5°C, respectively, during the coolest month. "Dry" and "Humid" locations were defined as having mean vapor pressure deficits above and below 1.0 kPa, respectively. The present study used data from seven of the original 12 locations to represent a range of temperatures (locations are included in Table S3). At Obregon and Tlaltizapan, Mexico normal and late sowing dates were used to provide contrasting temperature regimes at the same location. Of the sixteen genotypes originally included in the experiment, two were selected for the present study (cv Bacanora 88 and Nesser), which had low photoperiod sensitivity and low vernalization requirements. These two cultivars were selected for their low photoperiod sensitivity and low vernalization requirements to be comparable with the low to no vernalization requirements and photoperiod sensitivity of cv Yecora Rojo in the HSC experiment. Variables measured in the experiment included plants/m^2, biomass at 50% anthesis, days to 50% anthesis, days to physiological maturity, final biomass, grain yield, spikes/m^2, grains/spike, and kernel weight at maturity. Maturity dates for the late sown treatments for both cultivars at Tlaltizapan, Mexico were not available and therefore calculated using the average growing degree days from anthesis to maturity of all other treatments as an estimate.

All experiments were well watered and fertilized with temperature being the most important variable. Model inter-comparison was carried out using standardized protocols and one step of calibration. All sowing dates, anthesis and maturity dates, soil type characteristics and weather data were supplied to the modelers to simulate the CIMMYT experiments, but all other measurements were held back (blind).

Simulation outputs

The total-growing-season simulation outputs included: grain yield (t/ha), grains/m^2, kernel weight, above-ground biomass at maturity (t/ha), anthesis date and maturity date.

Data analysis

The root mean square relative error (RMSRE) between observed and simulated yield is calculated as:

$$\mathrm{RMSRE}_m = 100 \times \sqrt{\frac{1}{N}\sum_{i=1}^{N}\left(\frac{y_i - \hat{y}_{m,i}}{y_i}\right)^2} \qquad (1)$$

where y_i is the observed value of the *i*th measured treatment, $\hat{y}_{m,i}$ is the corresponding value simulated by model *m*, and *N* is the total number of treatments.

The coefficient of variation (CV%) of *x* represents the variation between models, calculated as:

$$CV\% = \frac{\sigma}{\bar{x}} * 100 \qquad (2)$$

where σ is the standard deviation of the variable (x), e.g. across models and $\bar{x}$ is their average.

The relative grain yield change in Fig. 1g and 3b was calculated as:

$$r_k = \frac{\bar{y}_{future,k} - \bar{y}_{baseline,k}}{\bar{y}_{baseline,k}} * 100 \qquad (3)$$

The box and whisker plots show the distributions. The horizontal line in each box represents the median response, the box delimits the 25^{th} to 75^{th} percentiles, and the whiskers extend from the 10^{th} to the 90^{th} percentile (Standard method). The Standard method uses a linear interpolation to determine the percentile values using the following approach; the data are sorted in increasing order from x_1, x_2, ….. x_n, then a parameter i is calculated as:

$$i = \frac{N * p_i}{100} + 0.5 \qquad (4)$$

where N is the total number of observations and p_i is a given percentile value. If the value of i is an integer then the corresponding data point x_i is the percentile. k is the largest integer less than i, and f=i-k.

The percentile value (v) is then calculated as:

$$v = f * x_{k+1} + (1 - f) * x_k \qquad (5)$$

We calculated the variability of yield due to year, model or location in the global impact assessment. Consider variability due to year (an equivalent procedure was used for variability due to model and location). First, we calculated the standard deviation of yield over years, for each combination of model and location, giving 900 standard deviations:

$$\sigma_{i,j}^{(Year)} = \sqrt{\mathrm{var}(Y \mid M_i, L_j)} \quad i = 1,...,30 \quad j = 1,...,30 \qquad (6)$$

where Y is yield and the notation $Y \mid M_i, L_j$ means yield for model M_i and location L_j. There are 30 values of $Y \mid M_i, L_j$ for each M_i and L_j since there are 30 years. The standard deviation above is the standard deviation over the 30 years. We then normalized those standard deviations by dividing by overall average yield, $\bar{Y}$, giving 900 coefficients of variation:

$$CV(\%)_{i,j}^{(Year)} = \frac{\sigma_{i,j}^{(Year)}}{\bar{Y}} * 100 \quad i = 1,...,30 \quad j = 1,...,30 \qquad (7)$$

The box plots in Figure 3a for each temperature represent those 900 CV values.

Calibration steps for each model for HSC experiment

The simulations were carried out by individual modelers in a ‘blind’ test (individual replicates were previously not publicly available (therefore called a “blind” analysis)) following AgMIP protocols[1]. Modelers had access to phenology and yield information of one treatment only (a treatment in the normal temperature range). Modelers could use this information to calibrate the cultivar (cv. Yecora for HSC experiment). For all other treatments, phenology, growth, LAI, yield and yield components were not made available. All presented simulations were carried out with these calibrated simulations. Only in a special exercise summarized in Table S4 and Figure S4, different levels of information was made available to analyze the impact of information availability on the model simulation results. Four steps with different levels of available information for model calibrations were carried out. Note, cultivar Yecora Rojo was used in all treatments in the HSC experiment for this special analysis.

A- Blind test: without calibration (modelers were supplied with daily weather data, crop management, qualitative information on cultivar (rating of photoperiod sensitivity and vernalization requirements), anthesis date and maturity date for one normal sowing date treatment).

B- Blind test with calibrated phenology: In addition to “A”, anthesis and maturity dates were supplied for all treatments to allow phenology calibration for the single cultivar used across all treatments.

C- Blind test with fixed phenology: Modelers were asked to fix their simulations to observed phenology across all treatments (i.e. simulated phenology errors were excluded).

D- Blind test with calibrated highest yield (normal temperature range): In addition to “A” and “B”, yield data for one treatment (normal temperature range with highest yield treatment was supplied. Models were allowed to be calibrated against yield data from one treatment only.

Blind test with calibrated highest yield (step D) was also applied to the CIMMYT data for each of the two cultivars. Models were allowed to be calibrated against anthesis and maturity dates and yield data from one treatment per cultivar only.

The individual model changes for each of these steps are shown in Supplementary Appendix Table SA1.

Climate series

Historical climate data were drawn from the AgCFSR climate dataset (http://data.giss.nasa.gov/impacts/agmipcf/). AgCFSR combines retrospective analyses, gridded meteorological station datasets, and remotely-sensed radiation and precipitation information to form a coherent daily time series with all variables needed for agricultural modeling. 1981-2010 temperature trends in AgCFSR are a manifestation of the gridded meteorological station datasets to which monthly values are pegged, and may therefore have slight positive or negative biases due to inconsistencies in station coverage and data availability over the period analyzed. The +2 and +4 °C scenarios were created by adjusting each day's maximum and minimum temperatures upward by that amount and then adjusting vapor pressures and related parameters to maintain the original relative humidity at the maximum temperature time of day.

Calculation of seasonal mean temperature

Seasonal mean air temperature used in Figure 1 was calculated from daily air temperature (T_t), which was derived from the sum of eight contributions of a cosine variation between maximum and minimum daily air temperatures[74].

$$T_{\mathrm{t}} = \frac{1}{8}\sum_{r=1}^{r=8}\left(T_{\mathrm{h}} - T_{\mathrm{b}}\right) \tag{8}$$

with

$$T_{\mathrm{h}}\left(r\right) = T_{\mathrm{min}} + f_r\left(T_{\mathrm{max}} - T_{\mathrm{min}}\right) \tag{9}$$

and

$$f_r = \frac{1}{2}\left(1 + \cos\frac{90}{8}\left(2r - 1\right)\right) \tag{10}$$

where r is an index for a particular 3-h period, T_b (°C) is the base temperature (0°C) and T_h (°C) is the calculated three hour temperature contribution to estimated daily mean temperature. Negative contributions of T_h were treated as zero.

Global temperature impact assessment

Thirty locations from key wheat growing regions in the world, including the field experimental sites of the CIMMYT experiment, were used for a global temperature impact assessment (Table S3). These 30 locations were chosen from representative wheat growing regions with irrigated or high rainfall wheat (simulated with no water or N limitations) representing about 70% of current global wheat production[75]. To carry out the global temperature impact assessment, with exclusive focus on temperature, region-specific cultivars were used. Observed local mean sowing, anthesis and maturity dates were supplied with qualitative information on vernalization requirements and photoperiod sensitivity for each cultivar and modelers were asked to sow at the supplied sowing dates and calibrate their cultivar parameters against the observed anthesis and maturity dates by considering the qualitative information on vernalization requirements and photoperiod sensitivity. All model simulations were executed by the individual modeling groups.

Impact of temperature trend

Temperature trends (growing season mean temperature) were calculated based on 30 years (1981-2010; Fig. S1) for each of the 30 global locations (Table S3, Fig. S1). The first eight locations in Table S3 are identical to the experimental locations of the HSC and the CIMMYT experiments. The reminder 22 locations were strategically chosen to represent irrigation and high-rainfall regions of main wheat producing regions.

For the yield trend calculation, the 30-model ensemble median yield for each year was used to calculate the linear yield trend across the 30 years per location. The yield trend per year (slope of linear regression) was multiplied by 10 for a yield trend per decade, and expressed as a percentchange by dividing the trend by the mean yield across the 30-year period and multiplying by 100.

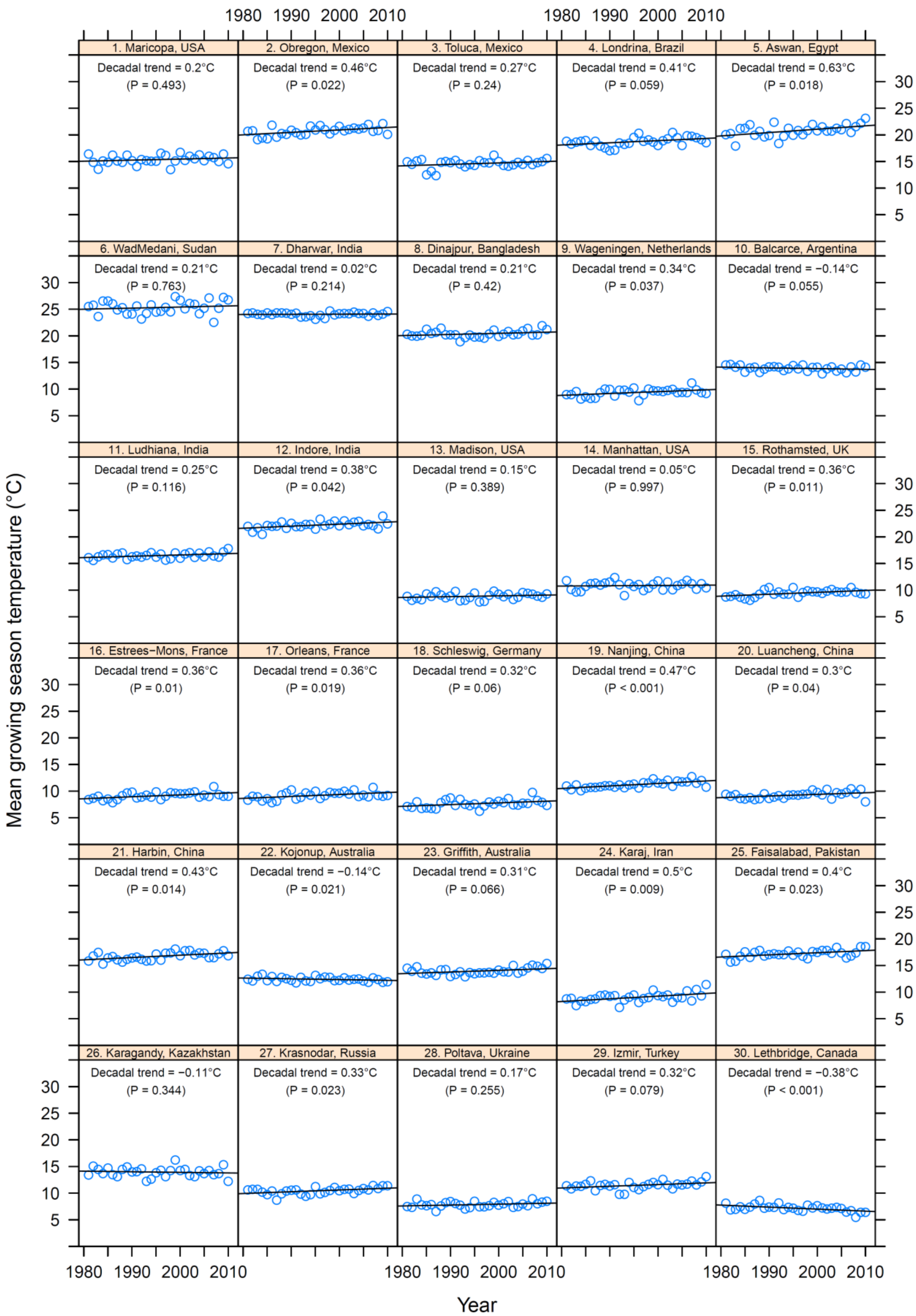

Supplementary Fig. S1. Measured growing season mean temperatures from 1981-2010 for each of the 30 global locations (Table S3) with linear trend line.

Disaggregating global temperature increase to regional temperature changes and extrapolating to global wheat production

Local grain yield impacts were expressed as an impact per ^{o}C local temperature change based on the +2^{o}C impact simulations. Global temperature increase (mean global temperature change) was disaggregated to regional temperature changes (Table S3, last column) via Figure 12-10 from the IPCC 2013 WG1 Report[76] as local temperature changes can be different to the global mean temperature change[76] (Table S3). The disaggregated local temperature changes per ^{o}C global mean temperature was then used to calculate the local temperature impact on grain yield and expressed as "grain yield impact per ^{o}C global mean temperature change".

The global wheat production impact was calculated using the following steps:

1) calculating the relative simulated mean yield impact for +2 ^{o}C of the 30 years (1981-2010) per single model at each location,

2) calculating the absolute regional production loss per single model by multiplying the relative yield loss from this model with the production represented at each location (using FAO country wheat production statistics of 2012 (www.fao.org)) and by multiplying with the specific local temperature factor twice from Table S3 [to account for the temperature impact from the simulations being for +2 ^{o}C and the local factor being for +1 ^{o}C globally in Table S3]; this assumes that the selected simulated location is representative for the entire wheat growing region surrounding this location,

3) adding up all regional production losses to the total global loss per single model,

4) calculating the relative change in global production (global production loss divided by current global production) and then dividing this by two (to normalize the simulated +2 ^{o}C impact to an impact per +1 ^{o}C change) per single model and

5) calculating the median, 25 and 75%tile relative global yield impact from the 30 model ensemble.

When using a different order of steps by first calculating the multi-model median before aggregating to global production loss, the median global impact is the same in both approaches (-6.0%). However, in the former approach used here, the 25 and 75%tiles are closer to the median

(-4.2% and -8.2% compared to -3.2% and -9.2% global production loss for 25 and 75%tiles in the latter mentioned approach, respectively).

Supplementary Table S3a. Locations, cultivars, growing season temperatures and local temperature changes per 1 °C of global temperature increase from key wheat growing locations in irrigated and high rainfall regions.

ID	Location	Country	Cultivar	Latitude	Longitude	Growing Season Temperature			
#	-	-	Name	Degree	Degree	Max	Min	Average	Delta+
1	Maricopa	USA	Yecora	33.06	-112.05	23.6	7.6	15.6	1.375
2	Obregon	Mexico	Tacupeto	27.33	-109.9	29.9	11.6	20.7	1.125
3	Toluca*	Mexico	Tacupeto	19.40	-99.68	21.2	7.5	14.4	1.125
4	Londrina	Brazil	Attila	-23.10	-51.13	25.6	14.1	19.9	1.125
5	Aswan	Egypt	Seri82	24.10	32.90	29.4	13.1	21.3	1.375
6	Wad Medani	Sudan	Debeira	14.40	33.50	35.0	17.1	26.1	1.375
7	Dharwar	India	Debeira	15.43	75.12	30.6	18.2	24.4	1.000
8	Dinajpur	Bangladesh	Kanchan	25.65	88.68	27.9	14.6	21.2	1.125
9	Wageningen	The Netherlands	Aminda	51.97	5.63	13.9	5.6	9.8	1.125
10	Balcarce	Argentina	Oasis	-37.75	-58.30	20.3	7.8	14.0	0.875
11	Ludhiana	India	HD2687	30.90	75.85	25.9	10.9	18.4	1.125
12	Indore	India	HI1544	22.72	75.86	30.3	14.3	22.3	1.125
13	Madison	Wisconsin, USA	Brigadier	43.93	-89.40	12.8	1.7	7.3	1.625
14	Manhattan	Kansas, USA	Fuller	39.14	-96.63	17.9	5.2	11.5	1.375
15	Rothamsted	UK	Avalon	51.82	-0.37	13.4	5.8	9.6	0.625
16	Estrées-Mons	NE France	Bermude	49.88	3.00	13.1	5.9	9.5	1.125
17	Orleans	Central France	Apache	47.83	1.91	14.4	5.8	10.1	1.125
18	Schleswig	Germany	Dekan	54.53	9.55	11.0	4.8	7.9	1.125
19	Nanjing	China	NM13	32.03	118.48	16.7	8.3	12.5	1.125
20	Luancheng	China	SM15	37.53	114.41	15.7	4.7	10.2	1.375
21	Harbin	China	LM26	45.45	126.46	22.1	10.8	16.5	1.375
22	Kojonup	Australia	Wyall	-33.84	117.15	18.5	7.0	12.7	0.875
23	Griffith	Australia	Avocet	-34.17	146.03	20.6	7.4	14.0	1.125
24	Karaj	Iran	Pishtaz	35.91	50.90	14.7	3.6	9.1	1.125
25	Faisalabad	Pakistan	Faisalabad	31.42	73.12	26.5	11.8	19.1	1.375
26	Karagandy	Kazakhstan	Steklov	50.17	72.74	18.9	5.7	12.3	1.375
27	Krasnodar	Russia	Brigadier	45.02	38.95	15.3	7.3	11.3	1.125
28	Poltava	Ukraine	Brigadier	49.37	33.17	11.6	3.3	7.5	1.125
29	Izmir	Turkey	Basri	38.60	27.06	17.9	8.3	13.1	1.125
30	Lethbridge	Canada	ACR	49.79	-112.83	11.7	-1.0	5.3	1.125

*The CIMMYT experimental site used in the model-observation comparison for location #3 was Tlaltizapan, Mexico (Lat 19.68 ; Lon -99.12, growing season mean temperature for maximum = 33.4 °C, minimum = 19.9 °C and average = 26.6 °C, about 100km north-east of Tuluca) outside any wheat growing regions. Therefore, Tuluca, Mexico was chosen for the global impact study, as a location in a wheat growing area.

+Local temperature delta per location for each degree of global temperature increase after Figure 12-10 from the IPCC 2013 WG1 Report[76].

Supplementary Table S3b. Locations, cultivars, sowing date, anthesis date and maturity date from key spring and winter wheat growing locations in irrigated and high rainfall regions.

ID	Location	Country	Cultivar	Sowing date	Mean 50%-anthesis date (+/- 1 week)	Mean physiological maturity (+/- 1 week)
1	Maricopa	USA	Yecora, SW, no/low vernalization requirement, no/low photoperiod sensitive	25 Dec	5 Apr	15 May
2	Obregon	Mexico	Tacupeto C2001 SW, low vernalization requirement, low photoperiod sensitive	1 Dec	15 Feb	30 Apr
3	Toluca	Mexico	Tacupeto C2001 SW, low vernalization requirement, low photoperiod sensitive	10 May	5 Aug	20 Sep
4	Londrina	Brazil	Atilla SW, low-medium vernalization requirement, low-medium photoperiod sensitive	20 Apr	10 Jul	1 Sep
5	Aswan	Egypt	Seri M 82 SW, low-medium vernalization requirement, low photoperiod sensitive	20 Nov	20 Mar	30 Apr
6	Wad Medani	Sudan	Debeira SW, low/ moderate vernalization requirement, low photoperiod sensitive	20 Nov	25 Jan	25 Feb
7	Dharwar	India	Debeira SW, low/moderate vernalization requirement, low photoperiod sensitive	25 Oct	15 Jan	25 Feb
8	Dinajpur	Bangla-desh	Kanchan SW, low vernalization requirement, low photoperiod sensitive	1 Dec	15 Feb	15 Mar
9	Wageningen	The Nether-lands	Aminda, WW, high vernalization requirement, high photoperiod sensitive	5 Nov	25 Jun	5 Aug
10	Balcarce	Argentina	Oasis, WW, high/moderate vernalization requirement, high/moderate photoperiod sensitive	5 Aug	25 Nov	25 Dec
11	Ludhiana	India	HD 2687 SW, no/low vernalization requirement, low /no	15 Nov	5 Feb	5 Apr

			photoperiod sensitive			
12	Indore	India	HI 1544 SW, no/low vernalization requirement, low /no photoperiod sensitive	25 Oct	25 Jan	25 Mar
13	Madison	Wisconsin, USA	Brigadier WW, high vernalization requirement, high photoperiod sensitive	15 Sep	15 Jun	30 Jul
14	Manhattan	Kansas, USA	Fuller Medium vernalization, medium photoperiod sensitivity	01 Oct	15 May	01 Jul
15	Rothamsted	UK	Avalon WW vernalization requirement moderate/low daylength photoperiod sensitive	15 Oct	10 Jun	20 Aug
16	Estrées-Mons	NE France	Bermude WW, high vernalization requirement (score: 2/9; ca. 50 days) - high photoperiod sensitivity (score: 2/9) Intermediate heading date (5.5/9) - TKW = 47 g (score: 6/9)	5 Oct	31 May	15 Jul
17	Orleans	Central France	Apache WW High/moderate vernalization requirement (score: 4/9; ca. 40 days) Moderate photoperiod sensitivity (score: 3/9) - Early heading date (7/9) - TKW = 42 g (score: 5/9)	20 Oct	25 May	7 Jul
18	Schleswig	Germany	Dekan WW, low photoperiod sensitivity, moderate or maybe high vernalization requirement	25 Sep	15 Jun	25 Jul
19	Nanjing	China	NM13 WW, mid- vernalization requirement, moderate photoperiod sensitivity	5 Oct	5 May	5 Jun
20	Luancheng	China	SM15 WW High vernalization requirement, moderate photoperiod sensitivity	5 Oct	5 May	5 Jun
21	Harbin	China	LM26 SW Very low vernalization	5 Apr	15 Jun	25 Jul

			requirement, moderate to high photoperiod sensitivity			
22	Kojonup	Australia	Wyallkatchem SW, low vernalization requirement. Moderate photoperiod sensitivity	15 May	5 Oct	25 Nov
23	Griffith	Australia	Avocet SW, low vernalization requirement, moderate photoperiod sensitivity	15 Jun	15 Oct	25 Nov
24	Karaj	Iran	Pishtaz, SW Low vernalization requirement, photoperiod sensitivity	1 Nov	1 May	20 Jun
25	Faisalabad	Pakistan	Faisalabad-2008 SW, no vernalization requirement, low photoperiod sensitivity	15 Nov	5 Mar	5 Apr
26	Karagandy	Kazakh-stan	Steklov.-24 SW, Low vernalization requirement, medium photoperiod sensitivity	20 May	1 Aug	15 Sep
27	Krasnodar	Russia	Brigadier WW, high vernalization requirement, high photoperiod sensitive	15 Sep	20 May	10 Jul
28	Poltava	Ukraine	Brigadier WW, high vernalization requirement, high photoperiod sensitive	15 Sep	20 May	15 Jul
29	Izmir	Turkey	Basri Bey SW, SW, medium vernalization requirement, medium photoperiod sensitivity	15 Nov	1 May	1 June
30	Lethbridge	Canada	ACR WW, high vernalization requirement, high photoperiod sensitive	10 Sept	10 Jun	25 July

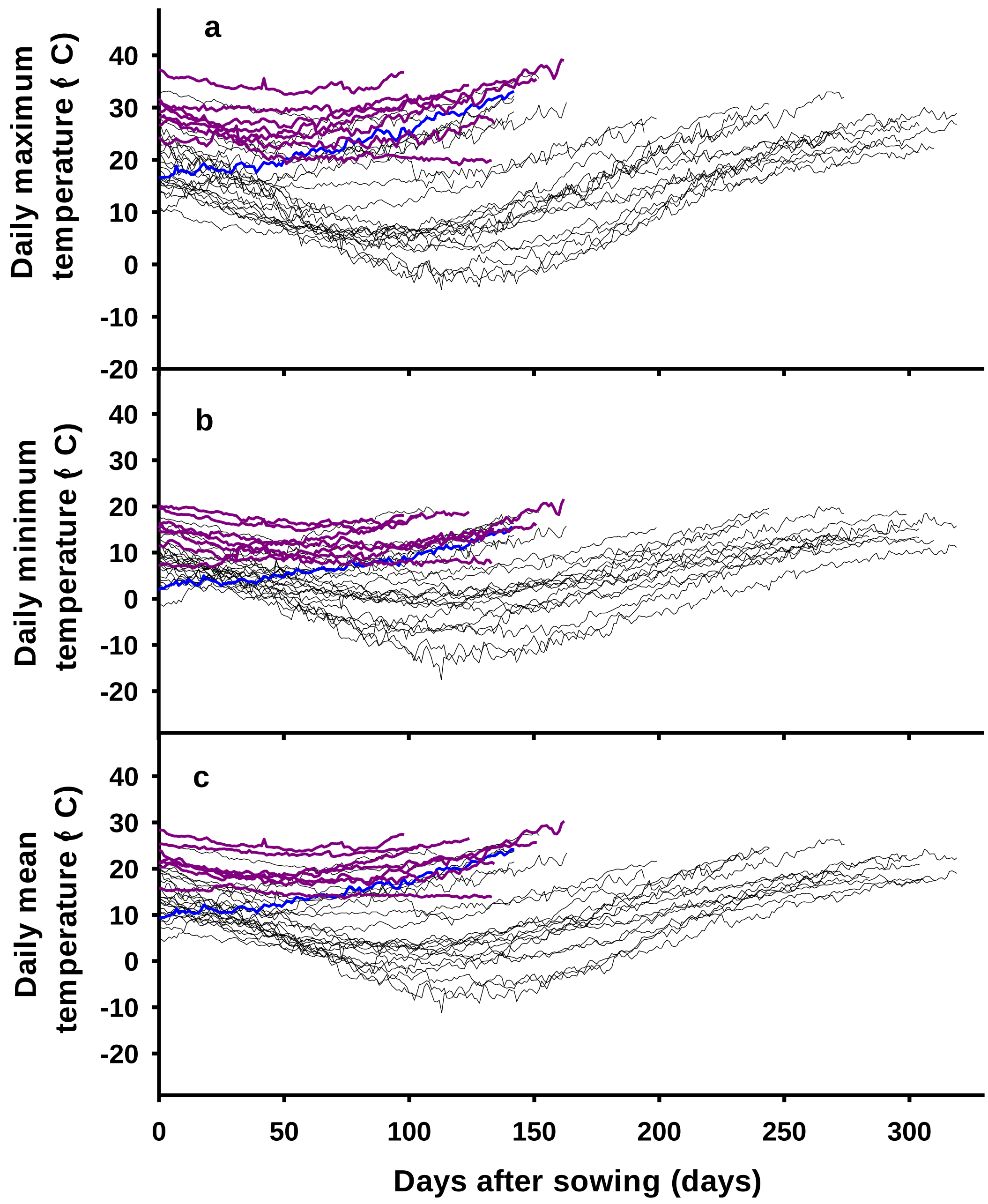

Supplementary Fig. S2. Daily 30-year averages (1981-2010) from sowing date to mean maturity dates for (**a**) T_{max}, (**b**) T_{min} and (**c**) mean temperatures. Maricopa (blue), seven CIMMYT locations (purple) and all other locations (black).

Supplementary Results

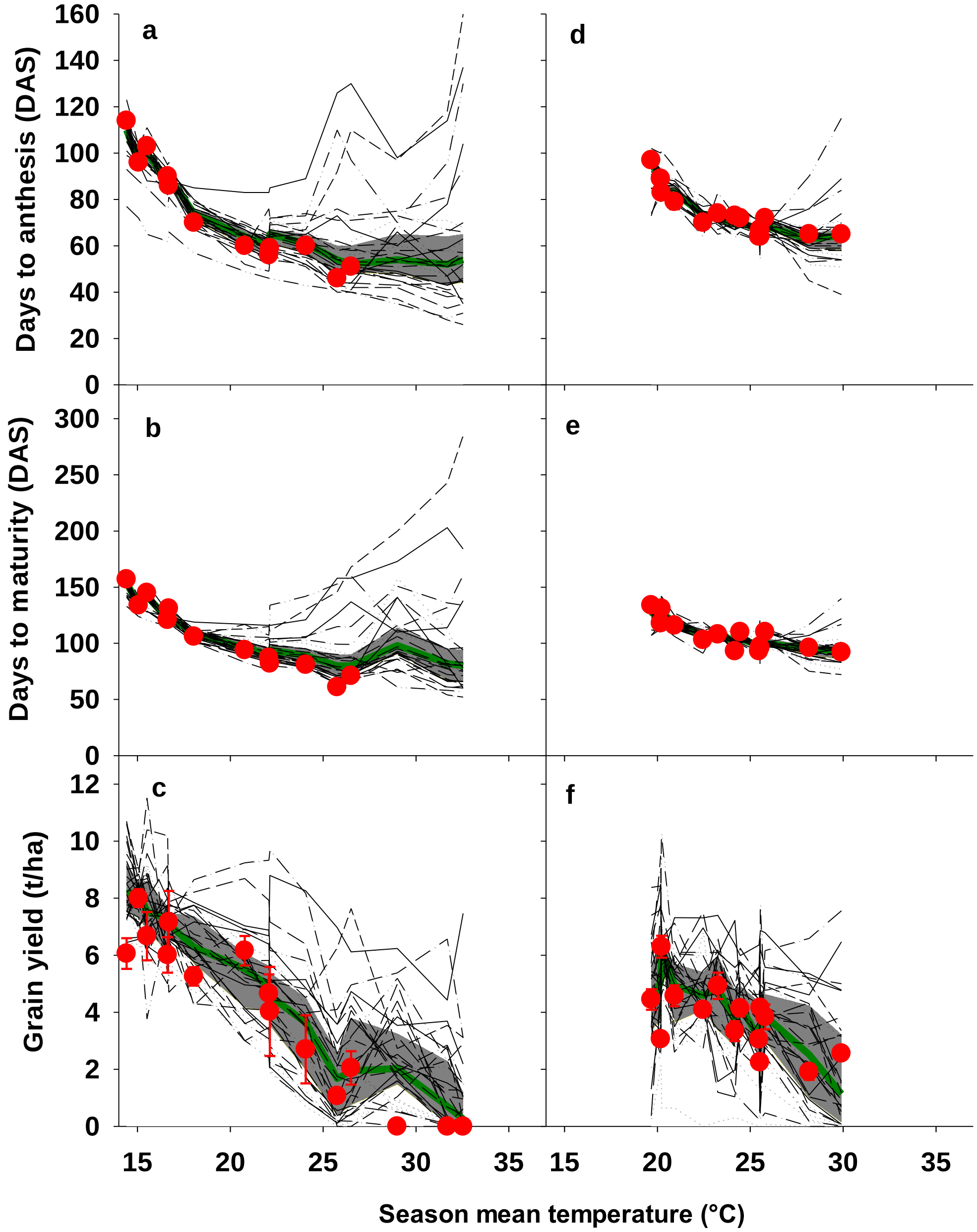

Supplementary Fig. S3. (**a** to **f**) Observed values ± 1 standard deviation (s.d.) are shown by red symbols with 30 simulated values shown by black lines (step D - calibrated highest yield). (**a** to **c**) Hot-Serial-Cereal experiment on *Triticum aestivum* L. cultivar Yecora Rojo with days-after-sowing (DAS), time-of-sowing and infrared heat treatments. (**d** to **f**) CIMMYT multi-environment temperature experiments on *T. aestivum* L. cultivar Bacanora with time-of-sowing treatments. Multi-model ensemble medians are shown by green lines. Intervals between the 25th and 75th percentiles are shaded gray. Error bars are not shown when smaller than symbol.

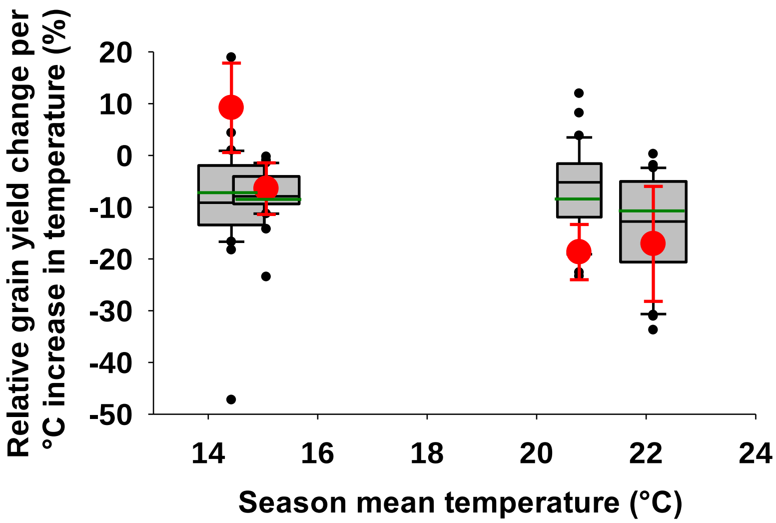

Supplementary Fig. S4. Relative grain yield change per °C temperature increase due to infrared heating for four treatments. Observed values ± 1 s.d. are shown by red symbols. Simulated outputs of 30 models are shown by box plots, where horizontal lines represent, from top to bottom, the 10th percentile, 25th percentile, median, 75th percentile and 90th percentile, and dots represent outliers.

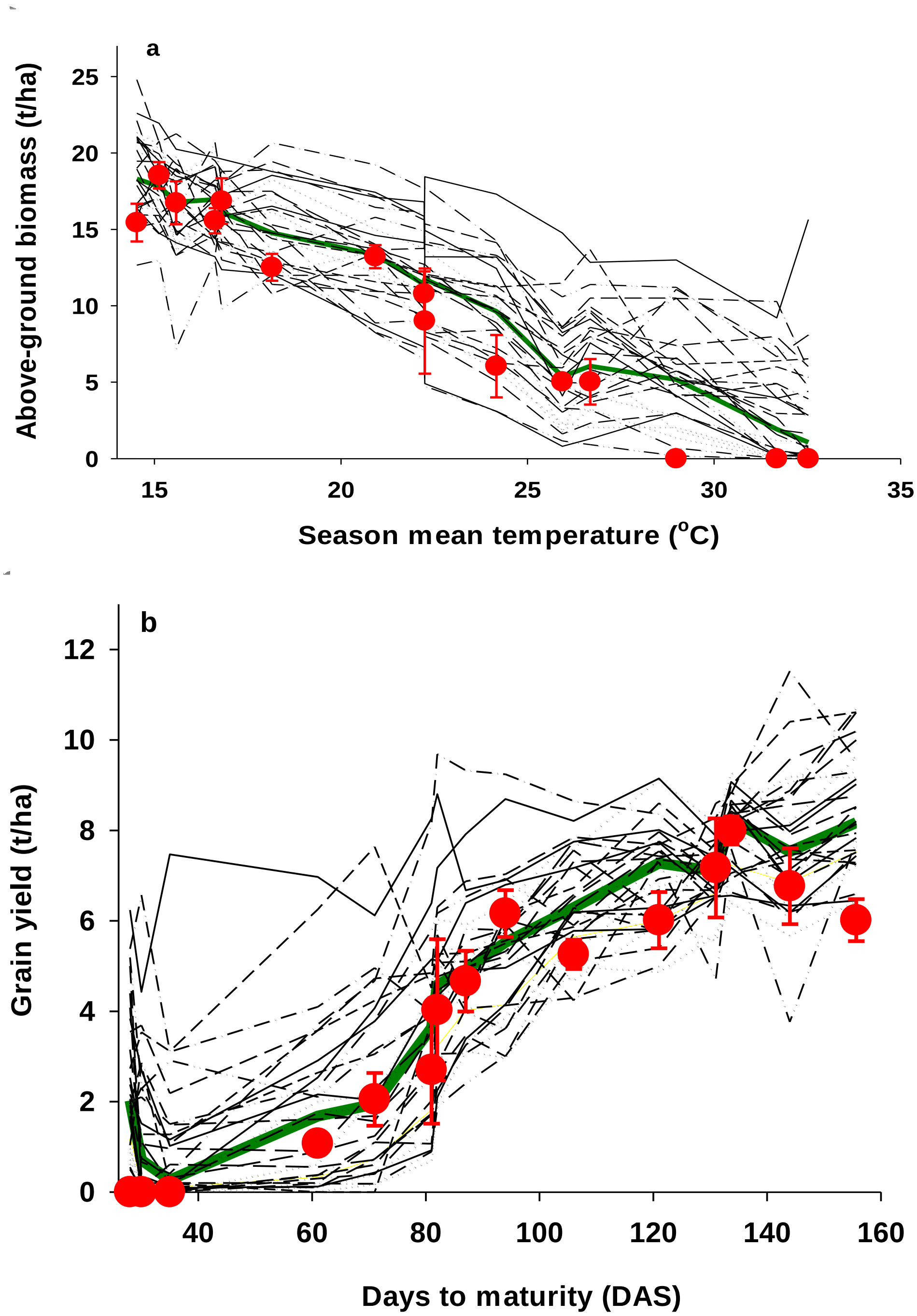

Supplementary Fig. S5. Observed mean (red circle) and 1 s.d. (red error bars) and simulated (black lines) (calibrated for highest yield treatment (step D)) for (**a**) above-ground biomass at maturity over mean season temperature and (**b**) grain yield over days to maturity of the Hot-Serial Cereal experiment for sowing dates and artificial heating. Note, the three dates with <40 days to maturity are the recorded dates of premature crop death with seasonal mean temperature >28 °C, with no recorded biomass and recorded zero grain yields. Multi-model ensemble median (green line) is shown. Space between 25th percentile and 75th percentile is shaded grey. Error bars are not shown when smaller than symbol.

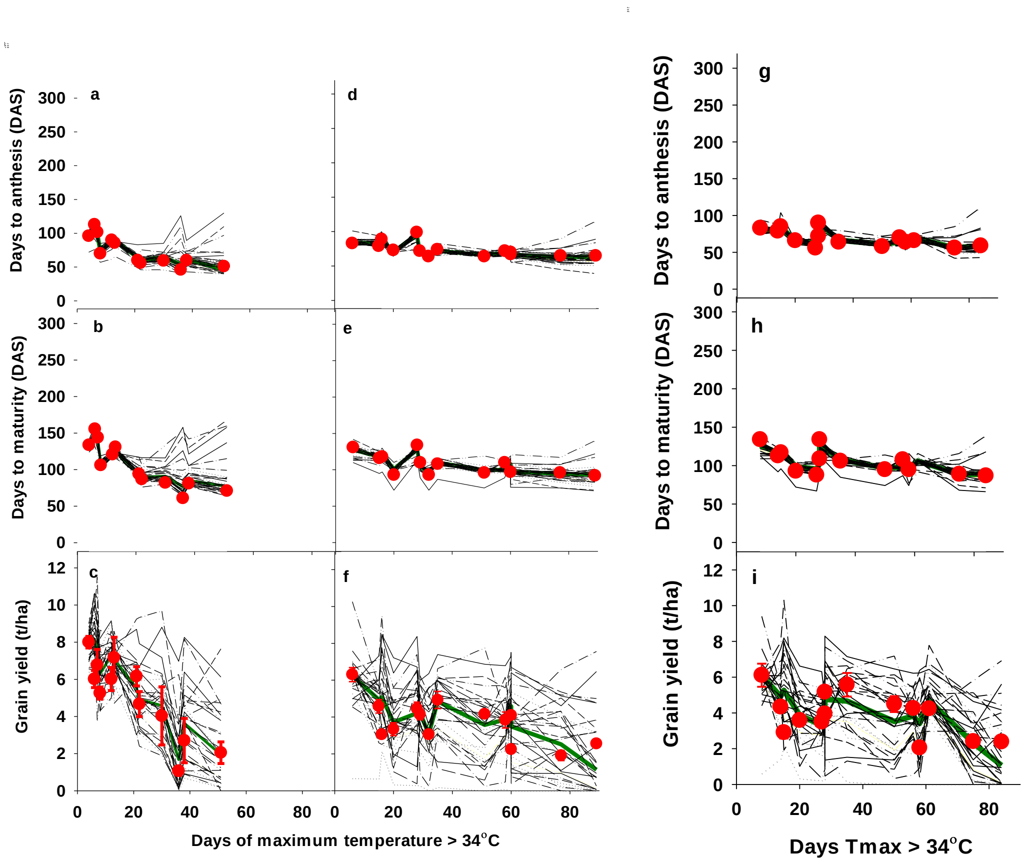

Supplementary Fig. S6. Observed (red symbols +/- 1 s.d.) and 30 simulated (black lines) (calibrated highest yield treatment (step D)) for a Hot-Serial-Cereal experiment (cultivar Yecora Rojo) with time-of-sowing and infra-red heating treatments for (**a**) days to anthesis, (**b**) days to maturity and (**c**) grain yields. Multi-temperature environment experiments from CIMMYT, including time-of-sowing treatments for cultivar Bacanora: (**d**) days to anthesis, (**e**) days to maturity and (**f**) grain yields and for cultivar Nesser: (**g**) days to anthesis, (**h**) days to maturity and (**i**) grain yields. Multi-model ensemble median (green line) is shown. Space between 25th percentile and 75th percentile is shaded grey. Error bars are not shown when smaller than symbol.

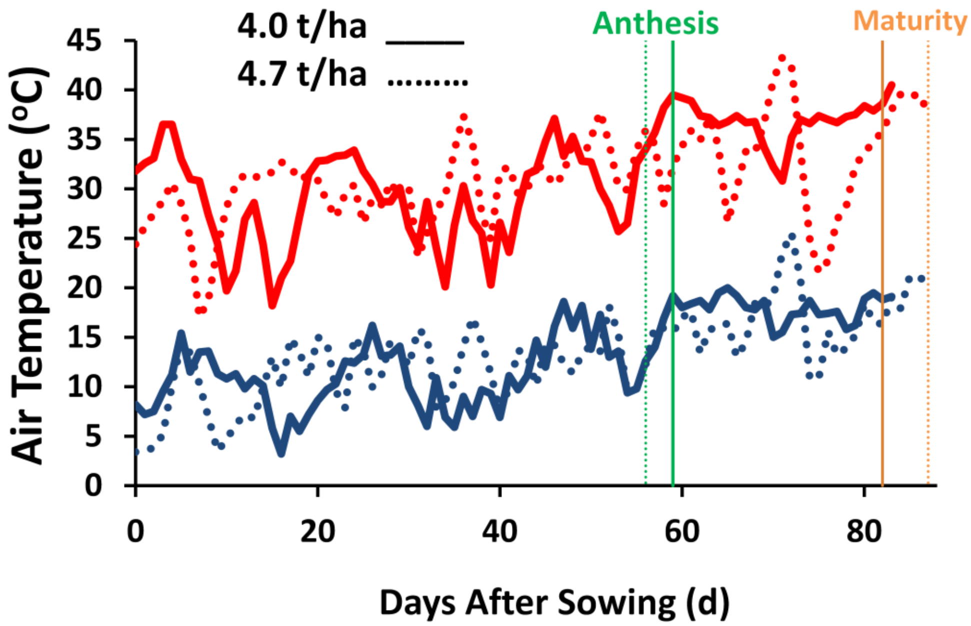

Supplementary Fig. S7. Measured daily temperatures (T_{max} in red and T_{min} in blue) for same mean seasonal temperature resulting in two different grain yields (4.7t/ha season ____ and 4.0 t/ha season - - -) of the Hot-Serial Cereal experiment. Anthesis and maturity dates are indicated with vertical lines.

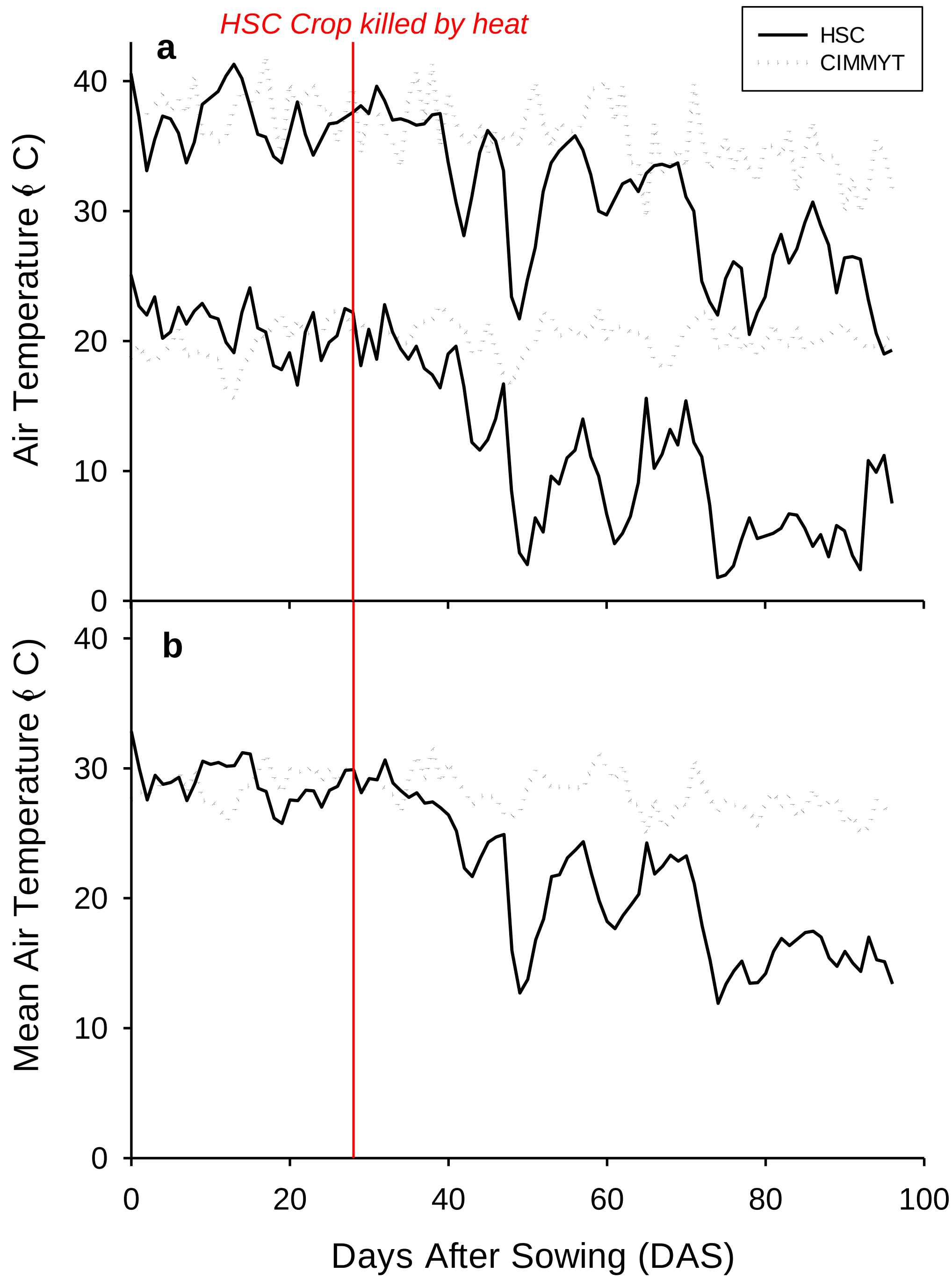

Supplementary Fig. S8. (**a**) Maximum and minimum and (**b**) mean daily temperatures for same growing season mean temperature of 28 ^{o}C for a Hot-Serial Cereal (HSC) experiment treatment with cv Yecora Rojo (growing season from sowing to pre-mature crop death at 28 days after sowing) and CIMMYT treatment with cv Bacanora (growing season from sowing to crop maturity at 96 days after sowing). Red vertical line indicates pre-mature death of crop in HSC treatment.

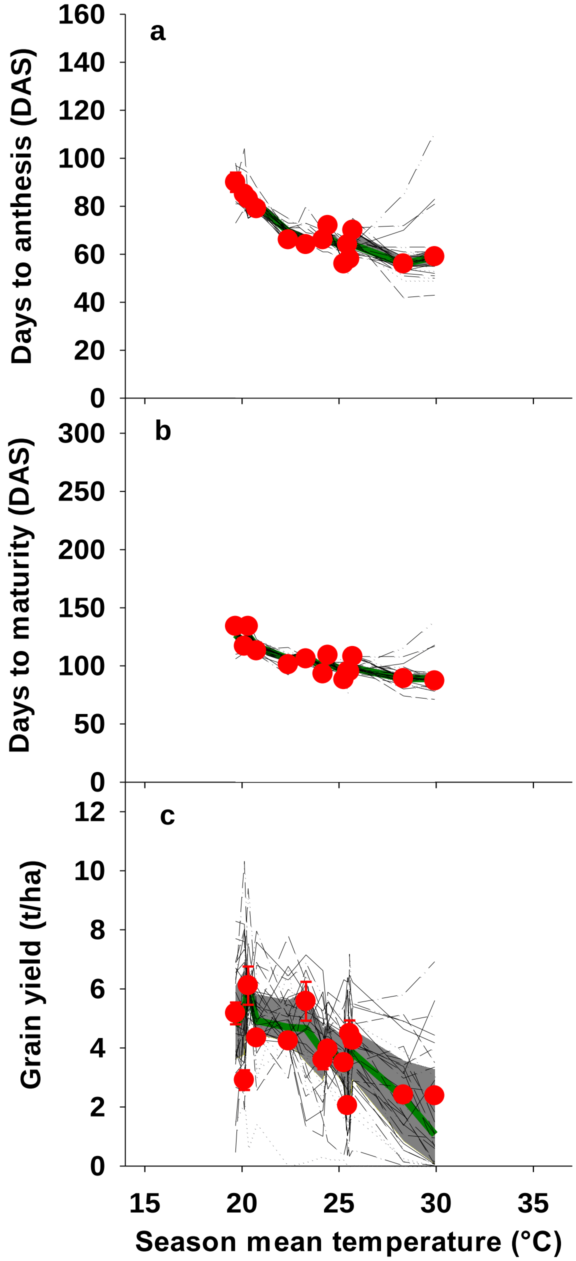

Supplementary Fig. S9. Observed (red symbols +/- 1 s.d.) and 30 simulated (black lines) for multi-temperature environment experiments from CIMMYT experiment (cultivar Nesser), including time-of-sowing treatments for (**a**) days to anthesis, (**b**) days to maturity and (**c**) grain yields. Multi-model ensemble median (green line) is shown. Space between 25th percentile and 75th percentile is shaded grey. Error bars are not shown when smaller than symbol.

Supplementary Table S4. Root Mean Square Relative Error (RMSRE %) of 30 crop simulation models grouped in quartiles (shown in red shades with quartile boundaries supplied in table above red shades) for simulated anthesis and maturity dates, and grain yields for **HSC** experiment: A- no calibration (Blind test), B- calibrated cultivar parameters across phenology dates (Calibrated phenology), C - fixed to observed phenology (i.e. simulated phenology errors excluded) (Fixed phenology), and D- calibrated cultivar for phenology and yield for highest observed yield treatment (Calibrated with highest observed yield).

	RMSRE (%)											
Percentiles / ensemble	**Days to anthesis**				**Days to maturity**				**Grain yield**			
	A	B	C	D	A	B	C	D	A	B	C	D
0%	4	3	0	3	4	3	0	3	20	21	21	24
25%	8	7	0	7	9	6	0	6	34	35	31	33
50%	13	9	0	10	13	11	0	10	48	45	44	44
75%	18	14	0	15	29	18	1	18	55	55	53	63
100%	73	73	2	73	75	64	5	64	112	166	92	184
e.median	8	7	0	7	12	10	0	11	11	14	21	24

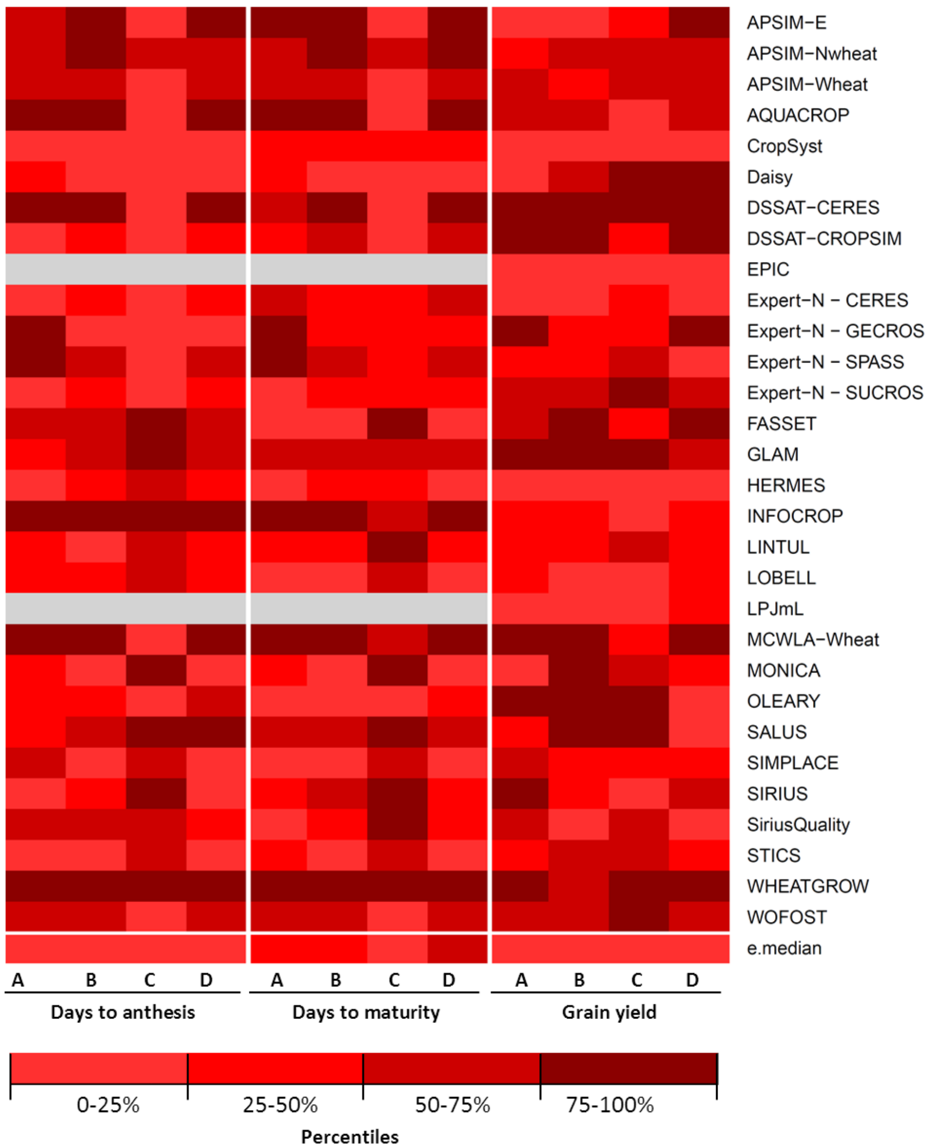

Supplementary Table S5. Root Mean Square Relative Error (RMSRE %) of 30 crop simulation models grouped in quartiles (shown in red shades with quartile boundaries supplied in table above red shades) for simulated anthesis and maturity dates, and grain yields for **CIMMYT** experiments for cultivar Bacanora and Nesser at seven locations.

Percentiles / ensemble	RMSRE (%) Days to anthesis		Days to maturity		Grain yield	
	Nesser	Bacanora	Nesser	Bacanora	Nesser	Bacanora
0%	0	1	1	2	28	22
25%	6	5	5	5	42	44
50%	7	7	6	6	52	53
75%	9	9	8	9	63	59
100%	28	24	20	101	97	106
e.Median	5	3	5	4	33	29

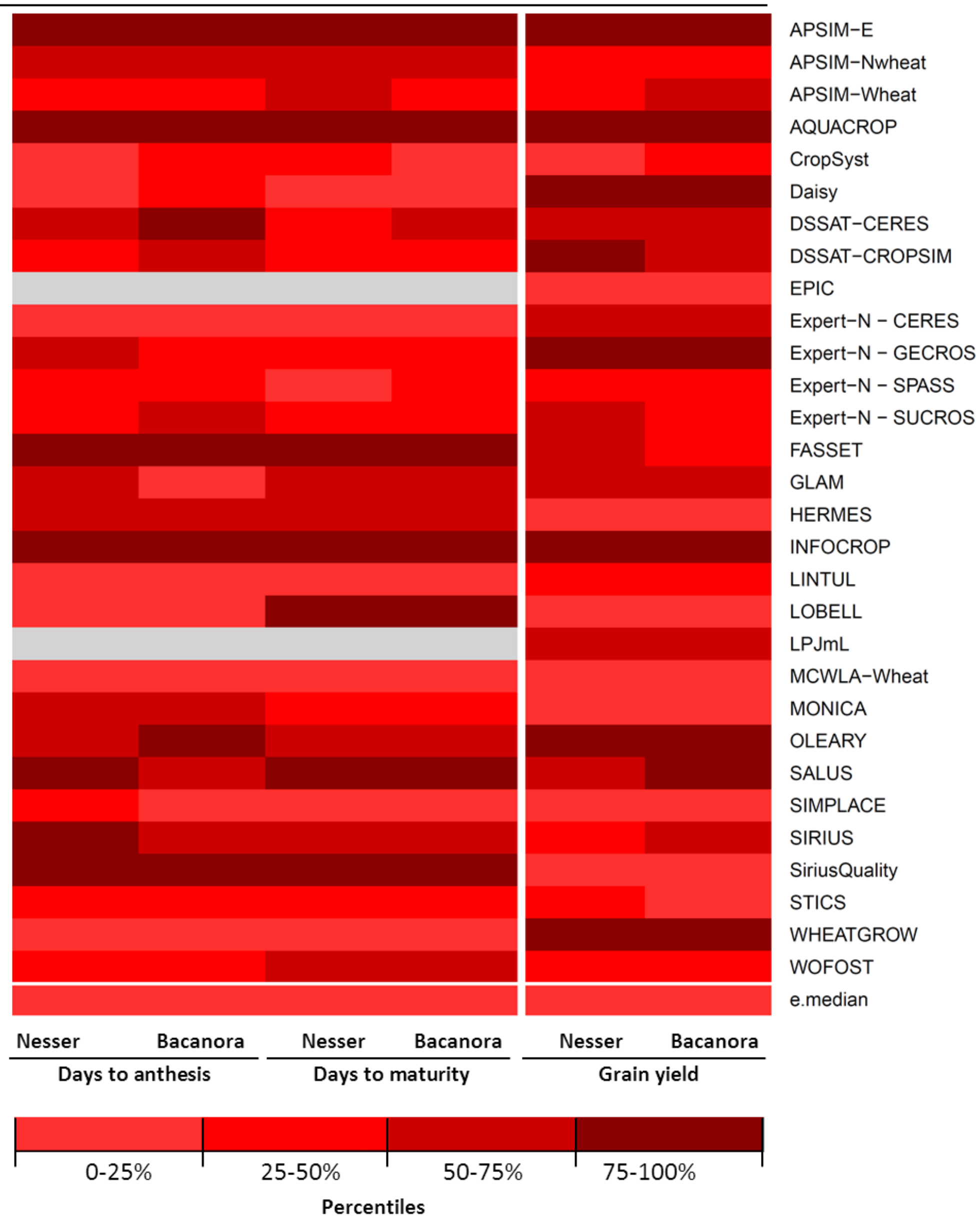

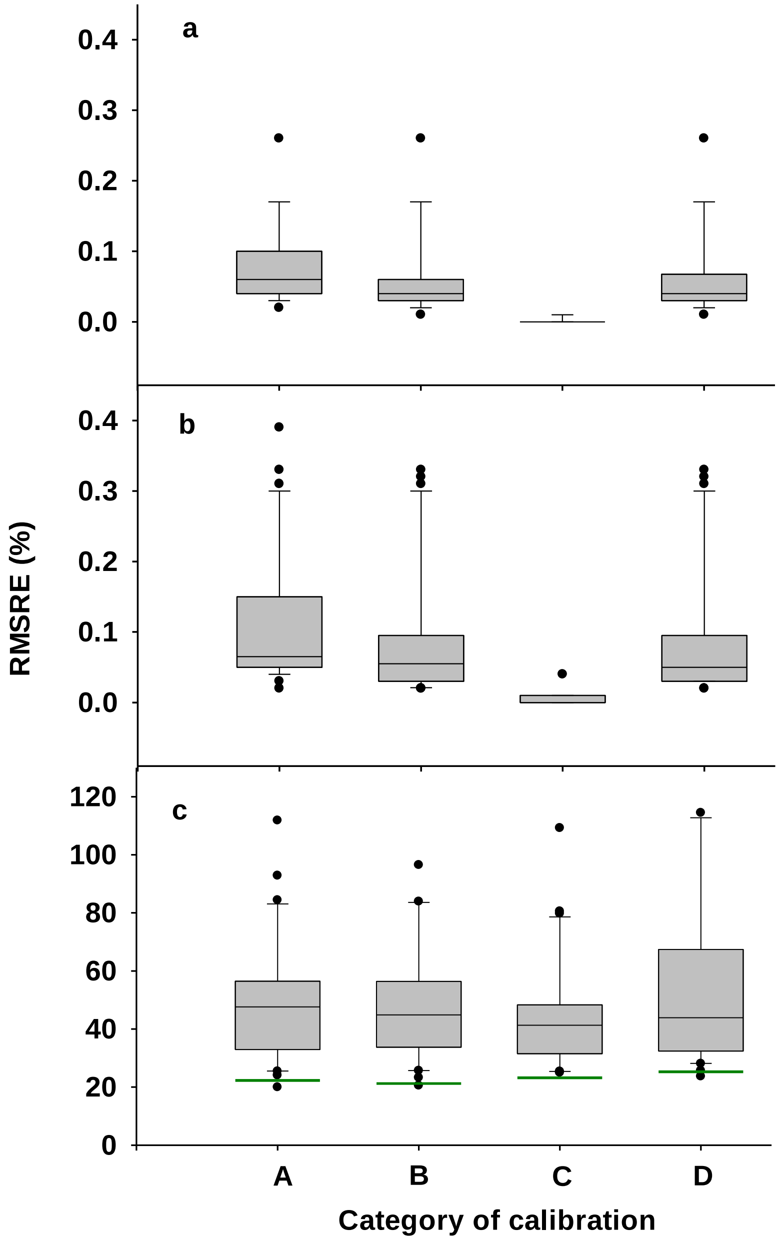

Supplementary Fig. S10. RMSRE (%) for 30 simulation models without calibration (step A- Blind test), calibrated cultivar parameters across phenology dates (step B- Blind test with calibrated phenology), simulations fixed to observed phenology (i.e. simulated phenology errors excluded) (step C- Blind test with fixed phenology) and calibrated cultivar for phenology and yield for one normal range temperature treatment with highest observed yield (step D- Blind test with calibrated highest yield) for (**a**) days from sowing to anthesis, (**b**) sowing to maturity and (**c**) grain yield. In each box plot, horizontal lines represent, from top to bottom, the 10^{th} percentile, 25^{th} percentile, median, 75^{th} percentile, 90^{th} percentile, and filled circles represent outliers, of 30 models. The RMSRE of the 30-model ensemble median (when used as a new predictor) is shown in (**c**) as a green horizontal line indicating the lowest errors.

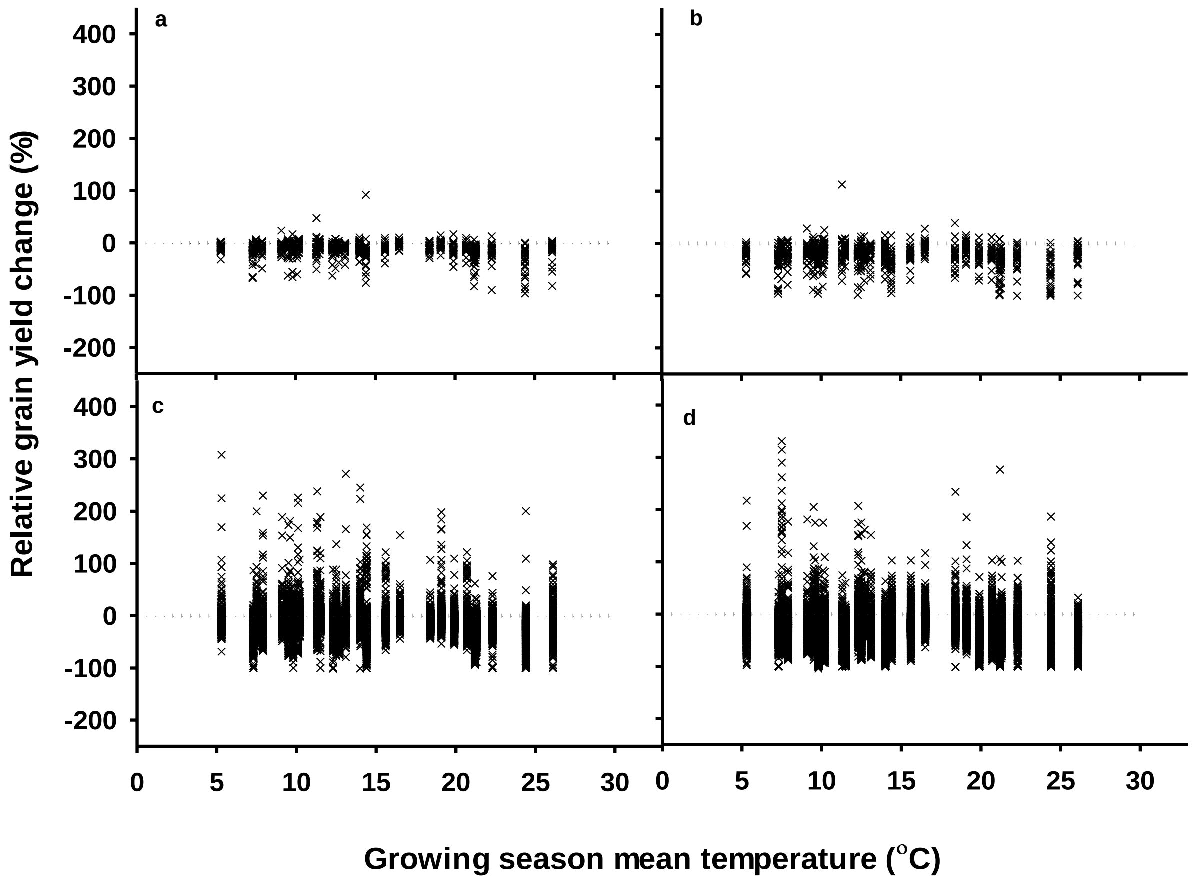

Supplementary Fig. S11. Simulated relative yield changes due to increasing temperature for 1981 to 2010 and 30 locations. (**a,b**) 30-year average yield change per location and (**c,d**) individual year grain yield changes per location with (**a,c**) +2 ^{o}C and (**b,d**) +4 ^{o}C temperature increase versus baseline growing season mean temperatures per location and season, respectively.

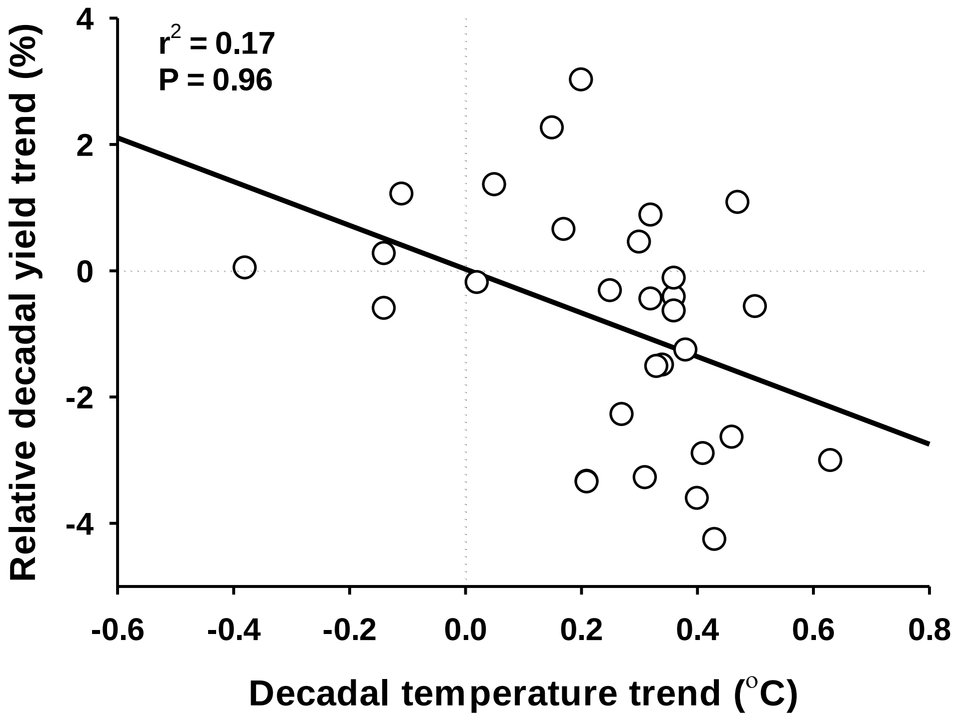

Supplementary Fig. S12. Relative decadal yield trend based on simulated 30-year model ensemble median annual yields versus local temperature trend between 1981 and 2010 for 30 global locations. Regression line (full line) and zero lines (dotted lines) are shown.

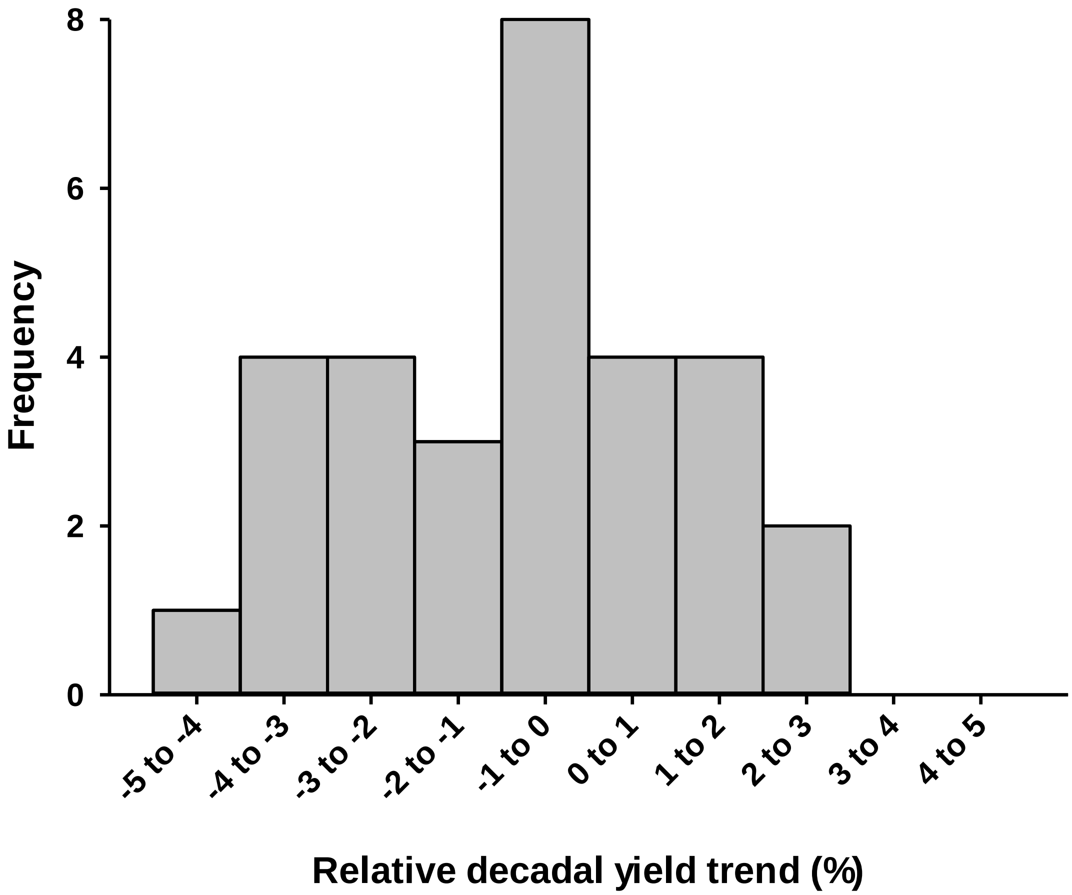

Supplementary Fig. S13. Frequency distribution of relative decadal yield change (%/decade) based on simulated 30-year model ensemble median annual yields between 1981 and 2010 for 30 global locations.

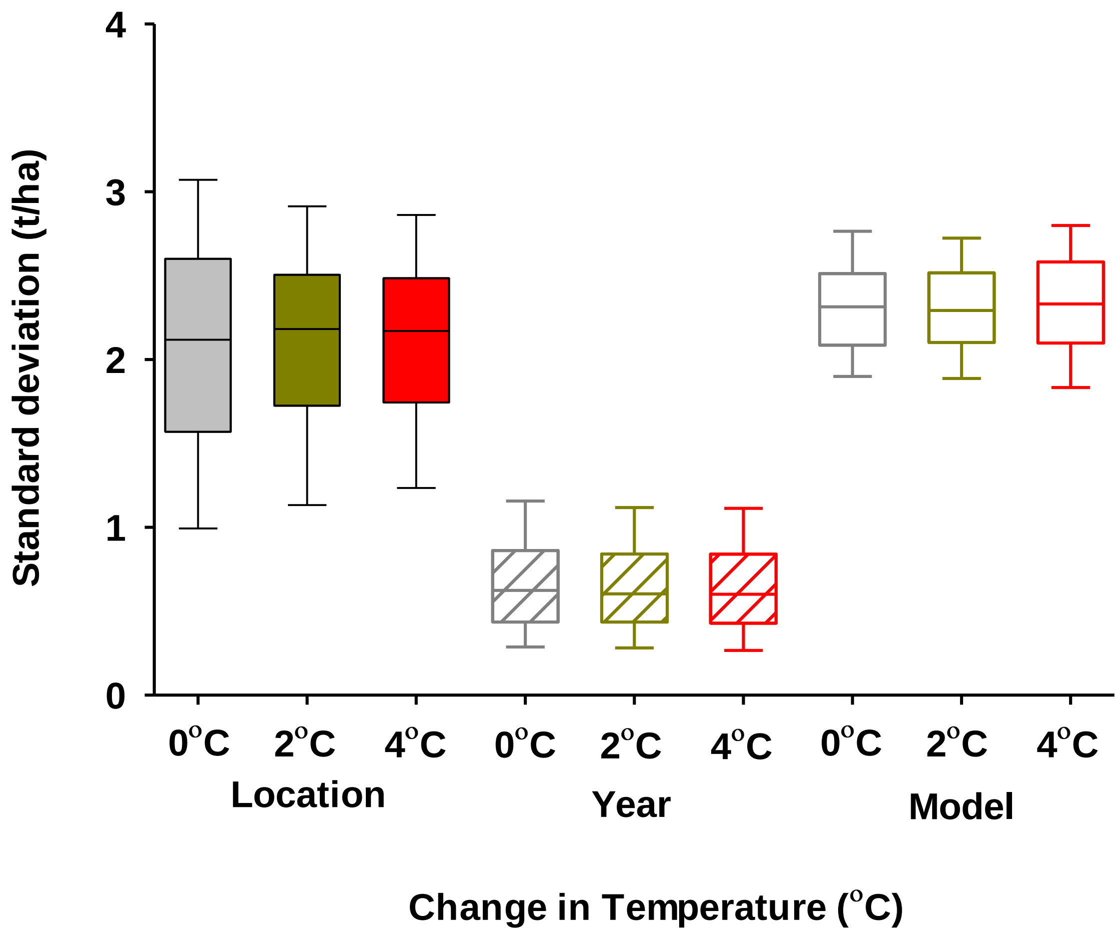

Supplementary Fig. S14. Standard deviation (s.d.) for simulated grain yields across locations and years and uncertainty due to crop models. In each box plot, horizontal lines represent, from top to bottom, the 10th percentile, 25th percentile, median, 75th percentile and 90th percentile of 900 simulations for current climate (baseline) (grey), +2 °C (green) and +4 °C (red).

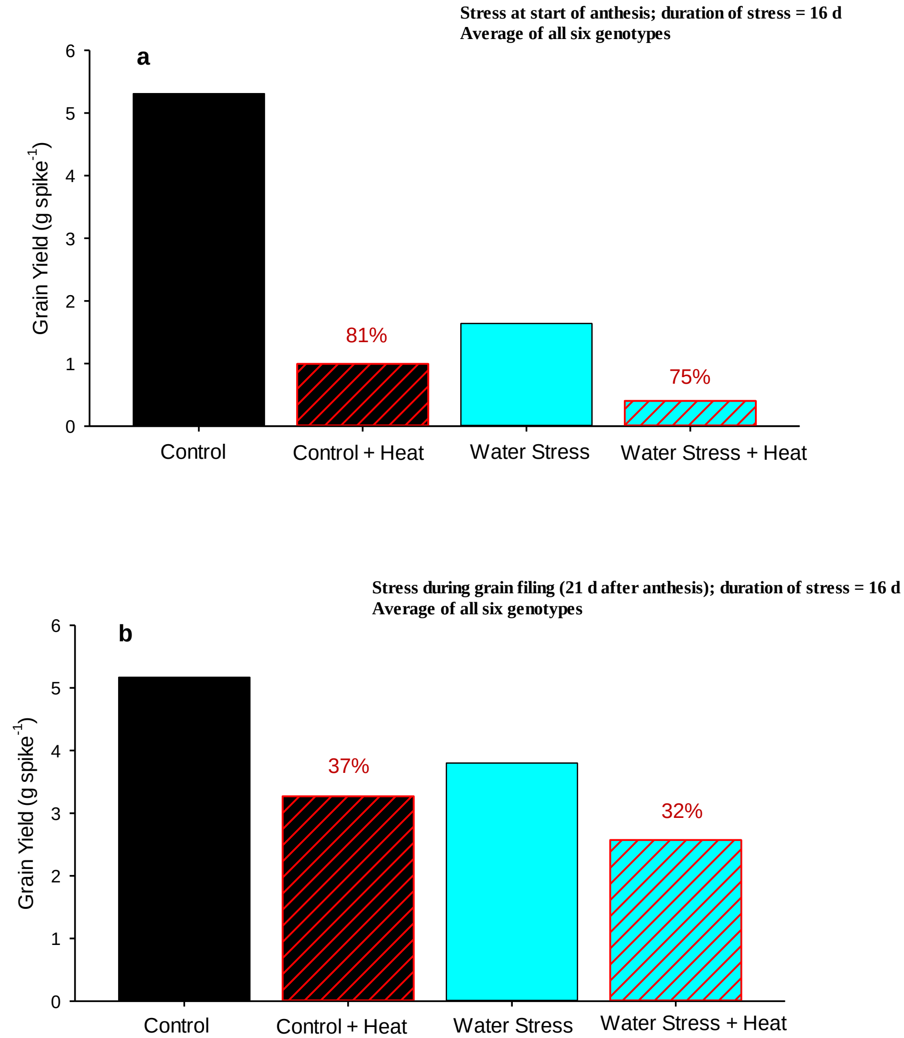

Supplementary Fig. S15. Measured mean (mean of six cultivars) wheat grain yield impact with increased temperatures (optimum day/night temperature of 21/15 ^{o}C and high temperature stress of 36/30 ^{o}C) with and without water stress for (**a**) 16 days of high temperature stress starting from anthesis and (**b**) for 16 days of high temperature stress during grain filling starting 21 days after anthesis. Note that g/spike represents grain yield as the number of spikes was not affected by the temperature treatment. Numbers indicate relative impacts due to increased temperatures. Re-calculated after Pradhan et al.[77].

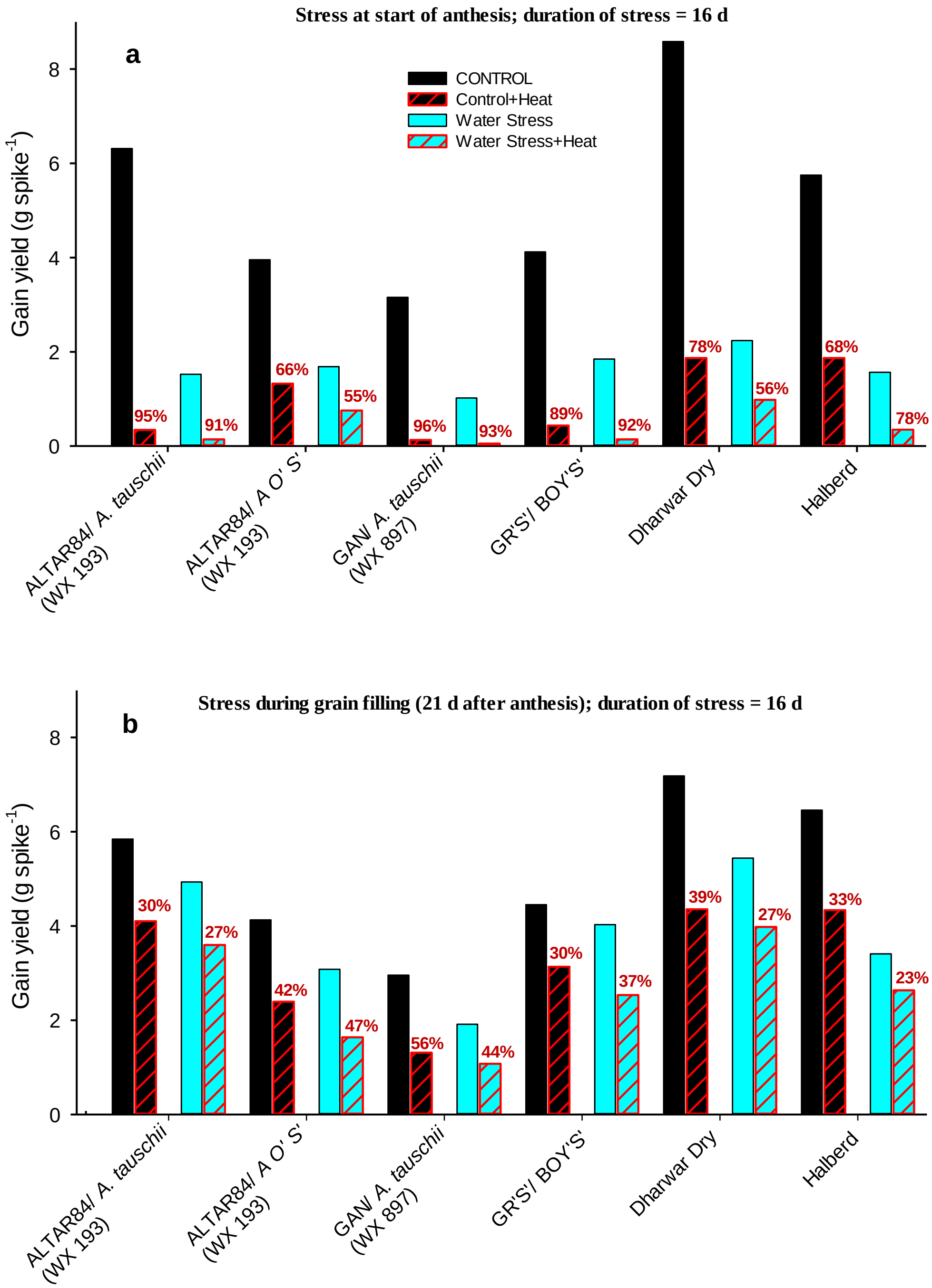

Supplementary Fig. S16. Measured wheat grain yield impact for six cultivars with increased temperatures (optimum day/night temperature of 21/15 ^{o}C and high temperature stress of 36/30 ^{o}C) with and without water stress for (**a**) 16 days of high temperature stress starting from anthesis and (**b**) for 16 days of high temperature stress during grain filling starting 21 days after anthesis. Note that g/spike represents grain yield as the number of spikes was not affected by the temperature treatment. Numbers indicate relative impacts due to increased temperatures. Re-calculated after Pradhan et al.[77].

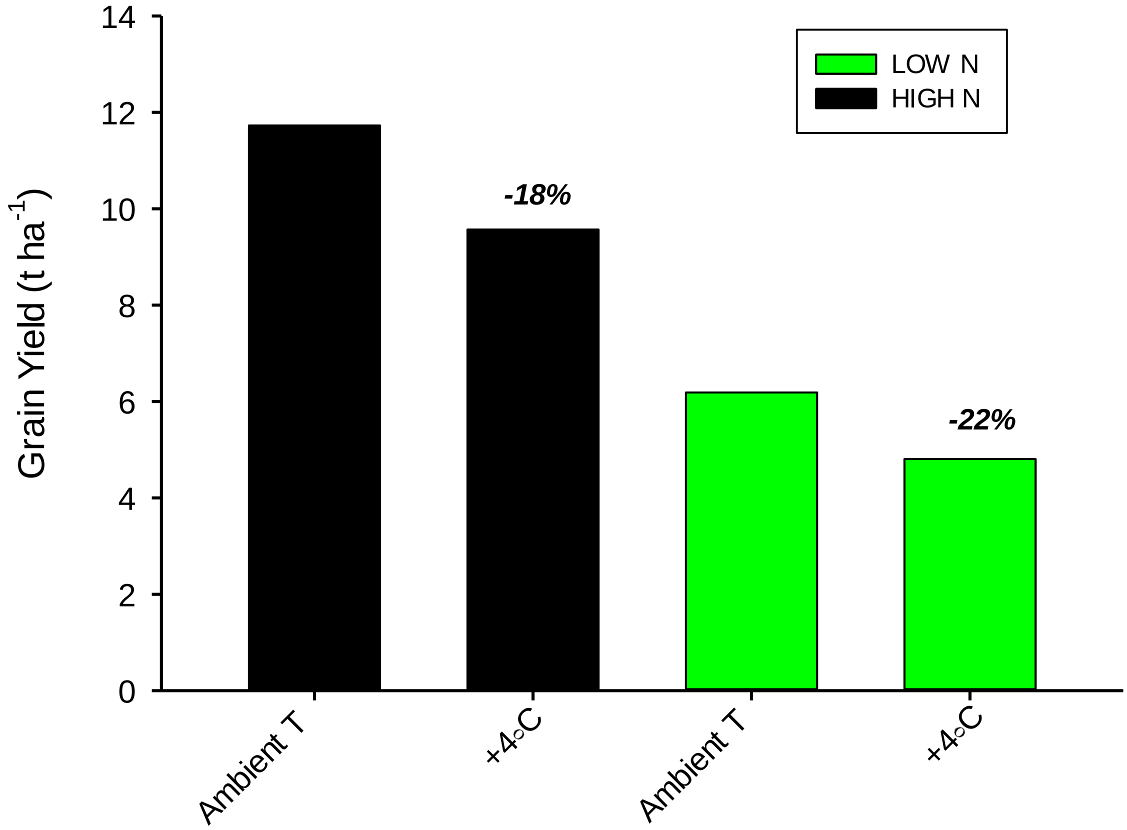

Supplementary Fig. S17. Measured mean wheat grain yield impact from increased temperatures for high N supply (black bars, 489 kg N/ha of fertiliser) and low N supply (green bars, 87 kg N/ha of fertiliser). Numbers indicate relative impacts due to increased temperatures. Re-calculated after Mitchell et al.[78].

Supplementary References

1. Rosenzweig, C. et al. The Agricultural Model Intercomparison and Improvement Project (AgMIP): Protocols and pilot studies. *Agricultural and Forest Meteorology* **170**, 166-182 (2013).
2. Ottman, M.J., Kimball, B.A., White, J.W. & Wall, G.W. Wheat Growth Response to Increased Temperature from Varied Planting Dates and Supplemental Infrared Heating. *Agronomy Journal* **104**, 7-16 (2012).
3. Wall, G.W., Kimball, B.A., White, J.W. & Ottman, M.J. Gas exchange and water relations of spring wheat under full-season infrared warming. *Global Change Biology* **17**, 2113-2133 (2011).
4. Keating, B.A. et al. An overview of APSIM, a model designed for farming systems simulation. *European Journal of Agronomy* **18**, 267-288 (2003).
5. Wang, E. et al. Development of a generic crop model template in the cropping system model APSIM. *European Journal of Agronomy* **18**, 121-140 (2002).
6. Chen, C., Wang, E. & Yu, Q. Modeling Wheat and Maize Productivity as Affected by Climate Variation and Irrigation Supply in North China Plain. *Agronomy Journal* **102**, 1037-1049 (2010).
7. Asseng, S. et al. Performance of the APSIM-wheat model in Western Australia. *Field Crops Research* **57**, 163-179 (1998).
8. Asseng, S. et al. Simulated wheat growth affected by rising temperature, increased water deficit and elevated atmospheric CO2. *Field Crops Research* **85**, 85-102 (2004).
9. Steduto, P., Hsiao, T., Raes, D. & Fereres, E. AquaCrop-The FAO Crop Model to Simulate Yield Response to Water: I. Concepts and Underlying Principles. *Agronomy Journal* **101**, 426-437 (2009).
10. Stockle, C., Donatelli, M. & Nelson, R. CropSyst, a cropping systems simulation model. *European Journal of Agronomy* **18**, 289-307 (2003).
11. Hansen, S., Jensen, H., Nielsen, N. & Svendsen, H. Simulation of nitrogen dynamics and biomass production in winter-wheat using the Danish simulation model DAISY. *Fertilizer Research* **27**, 245-259 (1991).
12. Hansen, S., Abrahamsen, P., Petersen, C.T. & Styczen, M. DAISY: model use, calibration, and validation. *Transaction of the ASABE* **55**, 1317-1335 (2012).
13. Hoogenboom, G. & White, J. Improving physiological assumptions of simulation models by using gene-based approaches. *Agronomy Journal* **95**, 82-89 (2003).
14. Jones, J. et al. The DSSAT cropping system model. *European Journal of Agronomy* **18**, 235-265 (2003).
15. Ritchie, J.T., Godwin, D.C. & Otter-Nacke, S. CERES-wheat: A user-oriented wheat yield model. Preliminary documentation (1985).
16. Hunt, L.A. & Pararajasingham, S. CROPSIM-wheat - a model describing the growth and development of wheat. *Canadian Journal of Plant Science* **75**, 619-632 (1995).
17. Kiniry, J. et al. EPIC model parameters for cereal, oilseed, and forage crops in the northern great-plains region. *Canadian Journal of Plant Science* **75**, 679-688 (1995).
18. Williams, J., Jones, C., Kiniry, J. & Spanel, D. The EPIC crop growth-model. *Transactions of the ASAE* **32**, 497-511 (1989).
19. Izaurralde, R.C., McGill, W.B. & Williams, J.R. in Managing agricultural greenhouse gases: Coordinated agricultural research through GRACEnet to address our changing climate (eds. Liebig, M.A., Franzluebbers, A.J. & Follett, R.F.) 409-429 (Elsevier, Amsterdam, 2012).
20. Priesack, E., Gayler, S. & Hartmann, H. The impact of crop growth sub-model choice on simulated water and nitrogen balances. *Nutrient Cycling in Agroecosystems* **75**, 1-13 (2006).
21. Ritchie, S., Nguyen, H. & Holaday, A. Genetic diversity in photosynthesis and water-use efficiency of wheat and wheat relatives. *Journal of Cellular Biochemistry*, 43-43 (1987).

22. Biernath, C. et al. Evaluating the ability of four crop models to predict different environmental impacts on spring wheat grown in open-top chambers. *European Journal of Agronomy* **35**, 71-82 (2011).
23. Stenger, R., Priesack, E., Barkle, G. & Sperr, C. (Land Treatment collective proceedings Technical Session, New Zealand, 1999).
24. Wang, E. & Engel, T. SPASS: a generic process-oriented crop model with versatile windows interfaces. *Environmental Modelling & Software* **15**, 179-188 (2000).
25. Yin, X. & van Laar, H.H. Crop systems dynamics: an ecophysiological simulation model of genotype-by-environment interactions (Wageningen Academic Publishers, Wageningen, The Netherlands, 2005).
26. Goudriaan, J. & Van Laar, H.H. (eds.) Modelling Potential Crop Growth Processes. Textbook With Exercises (Kluwer Academic Publishers, Dordrecht, The Netherlands, 1994).
27. Berntsen, J., Petersen, B., Jacobsen, B., Olesen, J. & Hutchings, N. Evaluating nitrogen taxation scenarios using the dynamic whole farm simulation model FASSET. *Agricultural Systems* **76**, 817-839 (2003).
28. Olesen, J. et al. Comparison of methods for simulating effects of nitrogen on green area index and dry matter growth in winter wheat. *Field Crops Research* **74**, 131-149 (2002).
29. Challinor, A., Wheeler, T., Craufurd, P., Slingo, J. & Grimes, D. Design and optimisation of a large-area process-based model for annual crops. *Agricultural and Forest Meteorology* **124**, 99-120 (2004).
30. Li, S. et al. Simulating the Impacts of Global Warming on Wheat in China Using a Large Area Crop Model. *Acta Meteorologica Sinica* **24**, 123-135 (2010).
31. Kersebaum, K. Modelling nitrogen dynamics in soil-crop systems with HERMES. *Nutrient Cycling in Agroecosystems* **77**, 39-52 (2007).
32. Kersebaum, K.C. Special features of the HERMES model and additional procedures for parameterization, calibration, validation, and applications. *Ahuja, L.R. and Ma, L. (eds.). Methods of introducing system models into agricultural research. Advances in Agricultural Systems Modeling Series 2, Madison (ASA-CSSA-SSSA)*, 65-94 (2011).
33. Aggarwal, P. et al. InfoCrop: A dynamic simulation model for the assessment of crop yields, losses due to pests, and environmental impact of agro-ecosystems in tropical environments. II. Performance of the model. *Agricultural Systems* **89**, 47-67 (2006).
34. Spitters, C.J.T. & Schapendonk, A.H.C.M. Evaluation of breeding strategies for drought tolerance in potato by means of crop growth simulation. *Plant and Soil* **123**, 193-203 (1990).
35. Shibu, M., Leffelaar, P., van Keulen, H. & Aggarwal, P. LINTUL3, a simulation model for nitrogen-limited situations: Application to rice. *European Journal of Agronomy* **32**, 255-271 (2010).
36. Gourdji, S.M., Mathews, K.L., Reynolds, M., Crossa, J. & Lobell, D.B. An assessment of wheat yield sensitivity and breeding gains in hot environments. *Proceedings of the Royal Society B-Biological Sciences* **280** (2013).
37. Bondeau, A. et al. Modelling the role of agriculture for the 20th century global terrestrial carbon balance. *Global Change Biology* **13**, 679-706 (2007).
38. Beringer, T., Lucht, W. & Schaphoff, S. Bioenergy production potential of global biomass plantations under environmental and agricultural constraints. *Global Change Biology Bioenergy* **3**, 299-312 (2011).
39. Fader, M., Rost, S., Muller, C., Bondeau, A. & Gerten, D. Virtual water content of temperate cereals and maize: Present and potential future patterns. *Journal of Hydrology* **384**, 218-231 (2010).

40. Gerten, D., Schaphoff, S., Haberlandt, U., Lucht, W. & Sitch, S. Terrestrial vegetation and water balance - hydrological evaluation of a dynamic global vegetation model. *Journal of Hydrology* **286**, 249-270 (2004).
41. Rost, S. et al. Agricultural green and blue water consumption and its influence on the global water system. *Water Resources Research* **44** (2008).
42. Müller, C. et al. Effects of changes in CO2, climate, and land use on the carbon balance of the land biosphere during the 21st century. *Journal of Geophysical Research-Biogeosciences* **112** (2007).
43. Tao, F., Yokozawa, M. & Zhang, Z. Modelling the impacts of weather and climate variability on crop productivity over a large area: A new process-based model development, optimization, and uncertainties analysis. *Agricultural and Forest Meteorology* **149**, 831-850 (2009).
44. Tao, F., Zhang, Z., Liu, J. & Yokozawa, M. Modelling the impacts of weather and climate variability on crop productivity over a large area: A new super-ensemble-based probabilistic projection. *Agricultural and Forest Meteorology* **149**, 1266-1278 (2009).
45. Tao, F. & Zhang, Z. Adaptation of maize production to climate change in North China Plain: Quantify the relative contributions of adaptation options. *European Journal of Agronomy* **33**, 103-116 (2010).
46. Tao, F. & Zhang, Z. Climate change, wheat productivity and water use in the North China Plain: A new super-ensemble-based probabilistic projection. *Agricultural and Forest Meteorology* **170**, 146-165 (2013).
47. Nendel, C. et al. The MONICA model: Testing predictability for crop growth, soil moisture and nitrogen dynamics. *Ecological Modelling* **222**, 1614-1625 (2011).
48. Oleary, G., Connor, D. & White, D. A simulation-model of the development, growth and yield of the wheat crop. *Agricultural Systems* **17**, 1-26 (1985).
49. OLeary, G. & Connor, D. A simulation model of the wheat crop in response to water and nitrogen supply .1. Model construction. *Agricultural Systems* **52**, 1-29 (1996).
50. OLeary, G. & Connor, D. A simulation model of the wheat crop in response to water and nitrogen supply .2. Model validation. *Agricultural Systems* **52**, 31-55 (1996).
51. Latta, J. & O'Leary, G. Long-term comparison of rotation and fallow tillage systems of wheat in Australia. *Field Crops Research* **83**, 173-190 (2003).
52. Basso, B., Cammarano, D., Troccoli, A., Chen, D. & Ritchie, J. Long-term wheat response to nitrogen in a rainfed Mediterranean environment: Field data and simulation analysis. *European Journal of Agronomy* **33**, 132-138 (2010).
53. Senthilkumar, S., Basso, B., Kravchenko, A.N. & Robertson, G.P. Contemporary Evidence of Soil Carbon Loss in the US Corn Belt. *Soil Science Society of America Journal* **73**, 2078-2086 (2009).
54. Angulo, C. et al. Implication of crop model calibration strategies for assessing regional impacts of climate change in Europe. *Agricultural and Forest Meteorology* **170**, 32-46 (2013).
55. Jamieson, P., Semenov, M., Brooking, I. & Francis, G. Sirius: a mechanistic model of wheat response to environmental variation. *European Journal of Agronomy* **8**, 161-179 (1998).
56. Jamieson, P. & Semenov, M. Modelling nitrogen uptake and redistribution in wheat. *Field Crops Research* **68**, 21-29 (2000).
57. Lawless, C., Semenov, M. & Jamieson, P. A wheat canopy model linking leaf area and phenology. *European Journal of Agronomy* **22**, 19-32 (2005).
58. Semenov, M. & Shewry, P. Modelling predicts that heat stress, not drought, will increase vulnerability of wheat in Europe. *Scientific Reports* **1** (2011).
59. Martre, P. et al. Modelling protein content and composition in relation to crop nitrogen dynamics for wheat. *European Journal of Agronomy* **25**, 138-154 (2006).

60. Ferrise, R., Triossi, A., Stratonovitch, P., Bindi, M. & Martre, P. Sowing date and nitrogen fertilisation effects on dry matter and nitrogen dynamics for durum wheat: An experimental and simulation study. *Field Crops Research* **117**, 245-257 (2010).
61. He, J., Stratonovitch, P., Allard, V., Semenov, M.A. & Martre, P. Global Sensitivity Analysis of the Process-Based Wheat Simulation Model SiriusQuality1 Identifies Key Genotypic Parameters and Unravels Parameters Interactions. *Procedia - Social and Behavioral Sciences* **2**, 7676-7677 (2010).
62. Brisson, N. et al. STICS: a generic model for the simulation of crops and their water and nitrogen balances. I. Theory and parameterization applied to wheat and corn. *Agronomie* **18**, 311-346 (1998).
63. Brisson, N. et al. An overview of the crop model STICS. *European Journal of Agronomy* **18**, 309-332 (2003).
64. Cao, W. & Moss, D.N. Modelling phasic development in wheat: a conceptual integration of physiological components. *Journal of Agricultural Science* **129**, 163-172 (1997).
65. Cao, W. et al. Simulating organic growth in wheat based on the organ-weight fraction concept. *Plant Production Science* **5**, 248-256 (2002).
66. Yan, M., Cao, W. & C. Li, Z.W. Validation and evaluation of a mechanistic model of phasic and phenological development in wheat. *Chinese Agricultural Science* **1**, 77-82 (2001).
67. Li, C., Cao, W. & Zhang, Y. Comprehensive Pattern of Primordium Initiation in Shoot Apex of Wheat. *ACTA Botanica Sinica*, 273-278 (2002).
68. Hu, J., Cao, W., Zhang, J., Jiang, D. & Feng, J. Quantifying responses of winter wheat physiological processes to soil water stress for use in growth simulation modeling. *Pedosphere* **14**, 509-518 (2004).
69. Pan, J., Zhu, Y. & Cao, W. Modeling plant carbon flow and grain starch accumulation in wheat. *Field Crops Research* **101**, 276-284 (2007).
70. Pan, J. et al. Modeling plant nitrogen uptake and grain nitrogen accumulation in wheat. *Field Crops Research* **97**, 322-336 (2006).
71. Boogaard, H. & Kroes, J. Leaching of nitrogen and phosphorus from rural areas to surface waters in the Netherlands. *Nutrient Cycling in Agroecosystems* **50**, 321-324 (1998).
72. Alderman, P. et al. Proceeding on Modeling wheat response to high temperature (CIMMYT, CIMMYT, El Batan, Mexico, 19-21 June 2013, Mexico, D.F. CIMMYT, 2013).
73. Reynolds, M.P., Balota, M., Delgado, M.I.B., Amani, I. & Fischer, R.A. Physiological and morphological traits associated with spring wheat yield under hot, irrigated conditions. *Australian Journal of Plant Physiology* **21**, 717-730 (1994).
74. Weir, A.H., Bragg, P.L., Porter, J.R. & Rayner, J.H. A winter wheat crop simulation model without water or nutrient limitations. *Journal of Agricultural Science* **102**, 371-382 (1984).
75. Reynolds, M. & Braun, H. in Proceedings of the 3rd International Workshop of Wheat Yield Consortium (eds. Reynolds, M. & Braun, H.) ix-xi (CIMMYT, CENEB, CIMMYT, Obregon, Sonora, Mexico, 2013).
76. Collins, M. et al. Long-term Climate Change: Projections, Commitments and Irreversibility. *Intergovernmental Panel on Climate Change*, 108 (2013).
77. Pradhan, G.P., Prasad, P.V.V., Fritz, A.K., Kirkham, M.B. & Gill, B.S. Effects of drought and high temperature stress on synthetic hexaploid wheat. *Functional Plant Biology* **39**, 190-198 (2012).
78. Mitchell, R.A.C., Mitchell, V.J., Driscoll, S.P., Franklin, J. & Lawlor, D.W. Effects of increased CO_2 concentration and temperature on growth and yield of winter-wheat at 2 levels of nitrogen application. *Plant Cell and Environment* **16**, 521-529 (1993).

Appendix A

Appendix Tables SA1. Models cultivar parameters.

Model	Parameter				Simulation Step				
	#	Name	Unit	Definition	A	B	C-min	C-max	D
APSIM-E	1	shoot_lag	°Cday	Time lag before linear coleoptile growth starts (deg days)	40	56	20	150	56
	2	shoot_rate	°Cday/mm	Growing deg day increase with depth for coleoptile (deg day/mm depth)	1.5	2.1	1.5	2.2	2.1
	3	tt_floral_initiation	°Cday	Thermal time between terminal spikelet and flowering	555	565	380	565	565
	4	vern_sens	-	Sensitivity to vernalization	1	1.1	0.2	1.5	1.1
	5	photop_sens	-	Sensitivity to photoperiod	1.2	1.1	0.5	1.5	1.1
	6	tt_start_grain_fill	°Cday	Thermal time of the duration of grain filling	660	600	20	900	600
	7	max_grain_size	g/grain	maximum grain size	0.05	-	0.05	0.05	0.045
APSIM-Nwheat	1	P5	°Cday	Thermal time grain filling	660	-	220	880	660
	2	PHINT	°Cday	Phyllochron	120	105	40	150	105
	3	Grno	kernel/g-stem	Coefficient of kernel number per stem weight at the beginning of grain filling	2.4	-	-	-	2.1
	4	Fillrate	kernel/g-stem	Maximum kernel growth rate	1.9	-	-	-	3
	5	Sowing	days	Moved sowing dates	-	-	0	12	-
APSIM-wheat	1	shoot_lag	°Cday	Thermal time germination to emergence where shoot elongation is slow	50	-	20	100	-
	2	tt_end_of_juvenile	°Cday	Thermal time end juvenile to floral initiation	425	-	280	515	-
	3	tt_floral_initiation	°Cday	Thermal time floral initiation to flowering	580	-	380	700	-
	4	startgf_to_mat	°Cday	Thermal time start grain fill to maturity	660	500	40	920	-
	5	tt_flowering	°Cday	Thermal time flowering	120	120	35	120	-
	6	grains_per_gram_stem	grain/g		24	-	-	-	29
	7	potential_grain_filling_rate	g/grain/day		-	0.0019	-	-	0.0022
AQUACROP	1	DAS to emergence	°Cday	Days from sowing to emergence	114	121	5	13	121
	2	DAS to flowering	°Cday	Days from sowing to flowering	1180	1288	43	121	1288
	3	DAS to maturity	°Cday	Days from sowing to maturity	1854	2064	58	176	2064
	4	DAS to maximum canopy cover	°Cday	Days from sowing to maximum canopy cover	-	-	-	-	700
CropSyst	1	Degree days to emergence	°Cday	Degree-days to emergence	85	-	55	160	85
	2	Degree days to end vegetative growth	°Cday	Degree-days to end vegetative growth	840	760	690	1040	700
	3	Degree days to anthesis	°Cday	Degree days to anthesis	940	860	790	1140	860

	4	Degree days to begin grain filling	^{0}Cday	Degree-days to begin grain filling	1050	960	925	1240	960
	5	Degree days begin canopy senescence	^{0}Cday	Degree-days to begin canopy senescence	1100	1060	1025	1340	760
	6	Degree days maturity	^{0}Cday	Degree-days to maturity	1510	1435	1150	1730	1435
DAISY	1	Fm	CO_2/m^2/hour	Maximum assimilation rate	4	-	-	-	5
	2	SpLAI	m^2/g DM	Specific leaf area	0.031	-	-	-	0.039
	3	LeafAIMod	-	Specific leaf area modifier	(0 1) (2 1)	-	-	-	(0.0 1) (1.17 0.29) (2.0 0)
	4	Leaf	-	Fraction of shoot assimilate that goes to the leafs	(0.00 0.82) (0.25 0.70) (0.51 0.55) (0.60 0.50) (0.72 0.23) (0.83 0.01) (0.95 0.00) (2.00 0.00)	-	-	-	(0.00 0.41) (0.87 0.95) (1 0.59) (1.25 0.00) (2.00 0.00)
	5	Stem	-	Fraction of shoot assimilate that goes to the stem	(0.00 0.18) (0.25 0.30) (0.51 0.45) (0.60 0.50) (0.72 0.77) (0.83 0.99) (0.95 1.00) (1.51 0.00) (2.00 0.00)	-	-	-	(0.00 0.59) (0.87 0.05) (1 0.40) (1.25 0.00) (2.00 0.00)
	6	E_Leaf	-	Conversion efficiency, leaf	0.68	-	-	-	0.79
	7	E_Stem	-	Conversion efficiency, stem	0.66	-	-	-	0.69
	8	E_SOrg	-	Conversion efficiency, storage organ	0.7	-	-	-	0.87
	9	ReMobilDS	-	Remobilization, Initial DS	1	-	-	-	1.3
	10	ReMobilRt	1/day	Remobilization, release rate	0.1	-	-	-	0.16
DSSAT-CERES	1	P1V	^{0}C	Optimum vernalizing temperature	5	0.2	0	10	0.2
	2	P1D	%reduction/h near threshold	Photoperiod response	32	0.5	0.5	117	0.5
	3	P5	^{0}Cday	Grain filling (excluding lag) phase duration	608	663	300	876	663
	4	G1	grain#/g	Kernel number per unit canopy weight at anthesis	24	-	-	-	19.7
	5	G2	mg/grain	Maximum grain size	60	-	-	-	41
	6	G3	Mg/day	Standard, non-stressed mature tiller weight (including grain)	3	-	-	-	0.3
	7	PHINT	^{0}Cday	Phyllocron	100	-	-	-	79
DSSAT-CROPSIM	1	GN_p_S	%	Standard grain nitrogen concentration	3	-	-	-	2.4
	2	P1	^{o}Cday	Duration of phase (1); germinate	390	360	380	380	370
	3	P2	^{o}Cday	Duration of phase (2); terminal spikelet	70	65	70	70	70

	4	P3	°Cday	Duration of phase (3); pseudo-stem	210	170	175	175	170
	5	P4	°Cday	Duration of phase (4); end leaf	185	160	165	165	160
	6	P5	°Cday	Duration of phase (5); heading	60	50	-	-	-
	7	P8	°Cday	Duration of phase (8); milk-dough	570	600	220	840	600
	8	PEMRG	°Cday per cm depth in soil	Emergence phase duration	10	-	20	15	10
	9	PGERM	Hydrothermal units	Phase duration, germination	10	-	20	15	8
	10	PHINT	°Cday	Phyllocron	80	100	100	100	100
	11	PPS1	% reduction in rate	Photoperiod sensitivity as % drop in rate	50	65	0	68	65
	12	TRGEM_0	°C	Base temperature, germination and pre-emergence growth rate	1	-	-3	-3	0
	13	TRGEM_1	°C	Optimal temperature (Topt1),germination and pre-emergence	26	-	-	-	20
	14	VEFF	-	Vernalization effect (rate reduction when unvernalized	0	0.3	-	-	-
	15	VREQ	day	Vernalization required for maximum development rate	15	2	0	35	8
EPIC	1	GMHU	°Cday	Thermal time between sowing and emergence	0	80	45	390	80
	2	PHU	°Cday	Thermal time between emergence and maturity	1380	1300	1085	1540	1300
	3	DMLA	-	Maximum potential LAI	6	-	-	-	9.31
	4	RLAD	-	LAI decline parameter (1 is linear, >1 accelerates, <1 retards decline rate)	1	-	-	-	1.46
	5	DLAI	-	Fraction of growing season when LAI declines	0.6	-	-	-	0.355
	6	DLAP1	-	First point on optimal LAI curve - Number before decimal is % of growing season, number after decimal is % of maximum LAI	15.01	-	-	-	17.15
	7	DLAP2	-	Second point on optimal LAI curve - Number before decimal is % of growing season, number after decimal is % of maximum LAI	50.95	-	-	-	43.99
	8	WA	-	Potential growth rate per unit of intercepted PAR	35	-	-	-	29.6
	9	HI	-	Harvest index	0.45	-	-	-	0.43
	10	CNY	-	Nitrogen fraction in yield	0.03	-	-	-	-
	11	BN1	-	Nitrogen fraction in plant at emergence	0.066	-	-	-	0.046
	12	BN2	-	Nitrogen fraction in plant at 0.5 maturity	0.025	-	-	-	0.02
	13	BN3	-	Nitrogen fraction in plant at maturity	0.015	-	-	-	0.01
Expert-N – CERES	1	G1	#grain/g	Grains per unit stem weight at	24	-	-	-	32.45

				anthesis					
	2	G2	mg/grain/d	Maximum grain filling rate	1.9	-	-	-	1.8
Expert-N – GECROS	1	LWLVR	1/day	Loss rate of leaf weight because of leaf senescence	0.01	-	-	-	0.03
	2	STEMNCMIN	g N/ g	Minimum N concentration in stems	0.01	-	-	-	0.0037
	3	LEAFNCMIN	g N/m	Minimum specific N concentration in leaves	0.35	-	-	-	0.261
	4	LNCI	g N/g	Initial leaf nitrogen concentration	0.054	-	-	-	0.06
	5	SLA	m^2/g	Specific leaf area	0.028	-	-	-	0.0264
Expert-N – SPASS	1	LUE	$g/J/m^2$	Light use efficiency	0.6	-	-	-	0.7
	2	G1	#grain/g	Number of grains per unit stem weight at anthesis	24	-	-	-	36
	3	G2	mg/grain/day	Maximum grain filling rate	1.9	-	-	-	1.6
	4	SpcLW	cm^2/g	Specific leaf weight	500	-	-	-	433
	5	Rext	cm/day	Maximum root extension rate	3	-	-	-	1.63
Expert-N – SUCROS	1	LUE	$g/J/m^2$	Light use efficiency	0.6	-	-	-	0.7
	2	G1	#grain/g	Number of grains per unit stem weight at anthesis	24	-	-	-	33
	3	SpcLW	cm^2/g	Specific leaf weight	500	-	-	-	385
FASSET	1	TTS0	°Cday	Thermal time between sowing and crop emergence	250	204	75	355	204
	2	TTS1	°Cday	Thermal time between crop emergence and anthesis	445	371	275	565	371
	3	TTS2	°Cday	Thermal time between anthesis and end of grain filling	388	536	250	720	536
	4	MaxGAI	m^2/m^2	Maximum crop green leaf area index	7	-	-	-	8
	5	LAIDM	m^2/g^1	Maximum ratio between LAI and DM in vegetative top part	0.011	-	-	-	0.015
	6	LAINratio	m^2/g^1	Maximum ratio between LAI and N in vegetative top part	0.4	-	-	-	0.6
	7	MaxAlloctoroot	-	Maximum fraction of DM production that is allocated to the root	0.6	-	-	-	0.3
	8	MaxNO$_3$UpRate	g N/m/day	Maximum uptake rate for nitrate-N	0.00006	-	-	-	0.0001
	9	MaxNH$_4$UpRate	G N/m/day	Maximum uptake rate for ammonium-N	0.0006	-	-	-	-
GLAM	1	GCPLFL	°Cday	Thermal time from emergence to anthesis	1205	1261	905	1515	-
	2	GCFLPF	°Cday	Thermal time from anthesis to grain filling	176	184	132	221	-
	3	GCPFEN	°Cday	Thermal time duration of grain filling	509	442	34	729	-
	4	GCENHA	°Cday	Thermal time from end of grain filling to harvest maturity	96	82	6	135	-
	5	DLDTMXA	-	maximum change in LAI after anthesis	0.1	0.006	0.006	0.1	-
	6	DHDT	-	Rate of change in harvest index	-	-	-	-	0.0175
	7	P_TRANS_MAX	cm/day	Maximum value of potential transpiration	-	-	-	-	0.8

HERMES	1	TS1	°Cday	Thermal time between sowing and crop emergence	140	165	80	295	140
	2	TS2	°Cday	Thermal time between crop emergence and double ridge	320	282	-	-	-
	3	TS3	°Cday	Thermal time between double ridge and heading	490	-	295	620	500
	4	TS5	°Cday	Thermal time between flowering and maturity	330	440	225	620	440
	5	Tbase1			1	0	-	-	-
	6	Tbase5			9	6	-	-	-
	7	mois	% avail. water	Soil moisture threshold in 0-10 cm layer where germination starts to be retarded (linear increase)	0	70	-	-	-
	8	dayl2	Hour	Daylength requirement for development between emergence and double ridge	0	15	-	-	-
	9	dlbase2	Hour	Daylength base for development between emergence and double ridge	0	5	-	-	-
	10	Lf_bio_ini	kg DM/ha	Leaf biomass at emergence	53	-	-	-	80
	11	rt_bio_ini	kg DM/ha	Root biomass at emergence	53	-	-	-	80
	12	SLA1	$m^2/m^2/kg$	Specific leaf area per dry weight at emergence	0.002	-	-	-	0.0037
	13	SLA2	$m^2/m^2/kg$	Specific leaf area per dry weight at double ridge	0.0017	-	-	-	0.0025
	14	part_lf2		Fraction of dry matter allocated to leaves at double ridge	0.6	-	-	-	0.7
	15	part_st2		Fraction of dry matter allocated to stems at double ridge	0.2	-	-	-	0.1
	16	part_lf3		Fraction of dry matter allocated to leaves at ear emergence	0.5	-	-	-	0.15
	17	part_st3		Fraction of dry matter allocated to stems at ear emergence	0.37	-	-	-	0.75
	18	part_rt3		Fraction of dry matter allocated to roots at ear emergence	0.13	-	-	-	0.1
INFOCROP	1	TTGERM	°Cday	Thermal time between sowing and crop emergence	37	42	23	90	30
	2	TTVG	°Cday	Thermal time between crop emergence and 50% flowering	1200	1120	350	1500	1100
	3	TTGF	°Cday	Thermal time for grain filling period (50% flowering to Physiological maturity)	975	1120	730	1320	1100
	4	POTGWT	mg/grain	Maximum potential grain mass	66.5	48	-	-	-
	5	GNOCF	-	Factor determining the grain number before anthesis	30000	-	30000	42000	30000
LINTUL	1	TSUM1	°Cday	Thermal time from emergence to anthesis	1130	1100	-	-	-

2	TSUM2	°Cday	Thermal time from anthesis to maturity	760	-	-	-	-
3	SLATB		Table with specific leaf area as a function of development stage (DVS)	0.00, 0.0022,	-	-	-	0.00, 0.0040,
				0.50, 0.0022	-	-	-	0.60, 0.0022,
				2.00, 0.0022	-	-	-	-
4	LAICR	-	Critical leaf area index for overshadowing	4	-	-	-	4.5
5	RUETB	g DM/MJ PAR	Light use efficiency table for biomass production as function of DVS	0.00, 3.00,	-	-	-	0.00, 3.30,
				1.00, 3.00,	-	-	-	-
				1.30, 3.00,	-	-	-	-
				2.00, 0.40	-	-	-	2.00, 0.40
6	FRTB	-	Table fraction of total dry matter to roots as a function of DVS	0.00, 0.60,	-	-	-	0.00, 0.50,
				0.40, 0.55,	-	-	-	0.50, 0.50,
				1.00, 0.00,	-	-	-	-
				2.00, 0.00	-	-	-	-
7	FLTB	-	Table fraction of above-gr. DM to leaves as a function of DVS	0.00, 1.00,	-	-	-	-
				0.33, 1.00,	-	-	-	-
				0.80, 0.40,	-	-	-	0.70, 0.40,
				1.00, 0.10,	-	-	-	1.00, 0.30,
				1.01, 0.00,	-	-	-	-
				2.00, 0.00	-	-	-	-
8	FSTB	-	Table fraction of above-gr. DM to stems as a function of DVS	0.00, 0.00,	-	-	-	-
				0.33, 0.00,	-	-	-	-
				0.80, 0.60,	-	-	-	0.70, 0.60,
				1.00, 0.90,	-	-	-	1.00, 0.70,
				1.01, 0.15,	-	-	-	1.01, 0.05,
				2.00, 0.00	-	-	-	-
		-	Table fraction of above-gr. DM to storage organs as a function of DVS	0.00, 0.00,	-	-	-	-
				0.80, 0.00,	-	-	-	-
				1.00, 0.00,	-	-	-	-
				1.01, 0.85,	-	-	-	1.01,

									0.95,
					2.00, 1.00	-	-	-	-
	9	RDRLTB	1/day	Table of relative death rate of leaves as a function of daily mean temperature	-10., 0.00,	-	-	-	-
					10., 0.02,	-	-	-	-
					15., 0.03,	-	-	-	-
					30., 0.05,	-	-	-	30., 0.03,
					50., 0.09	-	-	-	-
	10	RDRRTB	1/d	Table relative death rate of stems as a function of DVS	0.00, 0.000,	-	-	-	-
					1.50, 0.000,	-	-	-	-
					1.5001, 0.020,	-	-	-	1.5001, 0.025,
					2.00, 0.020	-	-	-	2.00, 0.025
	11	DVSDLT	-	Development stage above which death of leaves starts in dependence of mean daily temperature	1	-	-	-	1.1
LOBELL	1	beta_intercept	day	Intercept of model to predict days to heading	246.7	174.3	-	-	-
	2	beta_gdd_105d	day / °Cd	Coefficient on degree days for first 105 days after sowing, used to predict days to heading	-0.03905	-0.05193	-	-	-
	3	beta_dl_105d	°C	Coefficient on average day length for first 105 days after sowing, used to predict days to heading	-8.31896	-0.3399	-	-	-
	4	Tavg_veg	°C	Mean air temperature, vegetative stage	0.138721	-	-	-	-
	5	eval(tavg_veg^2)	°C	Quadratic term of mean air temperature, vegetative phase	-0.003574	-	-	-	-
	6	dtr_veg	°C	Diurnal temperature range, vegetative phase	0.103487	-	-	-	-
	7	tavg_rep	°C	Mean air temperature, reproductive phase	0.199767	-	-	-	-
	8	eval(tavg_rep^2)	°C	Quadratic term of mean air temperature, reproductive phase	-0.014297	-	-	-	-
	9	dtr_rep	°C	Diurnal temperature range, reproductive phase	-0.028752	-	-	-	-
	10	tavg_gf	°C	Mean air temperature, grain filling phase	-0.497589	-	-	-	-
	11	eval(tavg_gf^2)	°C	Quadratic term of mean air temperature, grain filling phase	0.007916	-	-	-	-
	12	dtr_gf	°C	Diurnal temperature range, grain filling phase	0.061284	-	-	-	-
	13	srad_veg	MJ/m^2/d	Shortwave radiation, vegetative	0.021968	-	-	-	-

				phase				
	14	srad_rep	$MJ/m^2/d$	Shortwave radiation, reproductive phase	-0.013403	-	-	-	-
	15	srad_gf	$MJ/m^2/d$	Shortwave radiation, grain filling phase	0.066979	-	-	-	-
	16	dl_veg	hour	Daylength, vegetative phase	-1.006823	-	-	-	-
	17	dl_rep	hour	Daylength, reproductive phase	0.54261	-	-	-	-
	18	dl_gf	hour	Daylength, grain filling phase	-0.139909	-	-	-	-
	19	vpd_veg	kPa	Vapor pressure deficit, vegetative phase	-0.001429	-	-	-	-
	20	vpd_rep	kPa	Vapor pressure deficit, reproductive phase	-0.005764	-	-	-	-
	21	vpd_gf	kPa	Vapor pressure deficit, grain filling phase	-0.004475	-	-	-	-
	22	year	-	Growing season	0.028822	-	-	-	-
	23	tavg_veg:vpd_veg	-	Interaction between mean air temperature and vapor pressure deficit, vegetative phase	0.000061	-	-	-	-
	24	tavg_rep:vpd_rep	-	Interaction between mean air temperature and vapor pressure deficit, reproductive phase	0.000461	-	-	-	-
	25	tavg_gf:vpd_gf	-	Interaction between mean air temperature and vapor pressure deficit, grain filling phase	0.000406	-	-	-	-
	26	eval(tavg_veg)^2:vpd_veg	-	Interaction between quadratic term of the mean air temperature and vapor pressure deficit, vegetative phase	-0.0000012	-	-	-	-
	27	eval(tavg_rep)^2:vpd_rep	-	Interaction between quadratic term of the mean air temperature and vapor pressure deficit, reproductive phase	-0.0000067	-	-	-	-
	28	eval(tavg_gf)^2:vpd_gf	-	Interaction between quadratic term of the mean air temperature and vapor pressure deficit, grain filling phase	-0.0000088	-	-	-	-
LPJmL	1	PHU	°Cday	Thermal time from sowing to maturity	2022	2060	1600	2392	2060
	2	ps	hour	Saturating photoperiod, it controls the calculation of the factor that reduces the daily heat units as response to photoperiod	20	14	-	-	-
	3	psens	-	Sensitivity to the photoperiod effect [0-1](1 means no sensitivity), it controls the calculation of the factor that reduces the daily heat units as response to photoperiod	1	0.8	-	-	-

	4	harvest index	-	Ratio between grain yield and DM	-	-	-	-	0.45
	5	LAImax	m^2/m^2	Maximum leaf area index	-	-	-	-	8
	6	fphu_c	-	Parameter that defines the shape of the leaf development curve during growing season 1	-	-	-	-	0.15
	7	fphu_k	0-	Parameter that defines the shape of the leaf development curve during growing season 2	-	-	-	-	0.4
	8	flaimax_k	-	Fraction of plant maximal LAI	-	-	-	-	0.97
	9	fphu_sen	-	Fraction of growing period at which LAI starts decreasing	-	-	-	-	0.5
	10	α-a	-	Factor to scale leaf-level biomass production to stand level	-	-	-	-	1
MCWLA-Wheat	1	RmaxVGP1	-	Maximum development rate per day from emergence to terminal spikelet initiation	0.018	0.016375	0.0155	0.0235	0.0165
	2	RmaxVGP2	-	Maximum development rate per day from terminal spikelet initiation to anthesis	0.019	0.0178	0.017	0.0495	0.0202
	3	RmaxRGP	-	Maximum development rate per day from anthesis to maturity	0.0305	0.03175	0.023	0.155	0.0298
	4	rmaxv1	-	Maximum daily development rate between emergence to terminal spikelet initiation	-	0.0165	-	-	-
	5	rmaxv2	-	Maximum daily development rate between terminal spikelet initiation to anthesis	-	0.0202	-	-	-
	6	rmaxr	-	Maximum daily development rate between anthesis to maturity	-	0.0298	-	-	-
	7	photos	-	Sensitivity to photoperiod	-	0.36	-	-	-
	8	Pc	-	Critical photopheriod	-	8	-	-	-
MONICA	1	pc_StageTemperatureSum[1]	°Cday	Thermal time between sowing and crop emergence	148	158.3	80	205	-
	2	pc_StageTemperatureSum[2]	°Cday	Thermal time between emergence and double ridge	284	-	-	-	-
	3	pc_StageTemperatureSum[3]	°Cday	Thermal time between double ridge and begin flowering	510	383.33	330	760	-
	4	pc_StageTemperatureSum[4]	°Cday	Thermal time between begin flowering and full flowering	200	150	200	200	-
	5	pc_StageTemperatureSum[5]	°Cday	Thermal time duration of grain filling	660	507.86	222	570	-
	6	pc_StageTemperatureSum[5]	°Cday	Thermal time duration of senescence	25	-	-	-	-
	7	pc_BaseTemperature[1]	°Cday	Base temperature between sowing and crop emergence	1	-2.96	1	1	-
	8	pc_BaseTemperature[2]	°Cday	Base temperature between emergence and double ridge	1	-	-	-	-

	9	pc_BaseTemperature[3]	°Cday	Base temperature between double ridge and begin flowering	1	-1.22	1	1	-
	10	pc_BaseTemperature[4]	°Cday	Base temperature between begin flowering and full flowering	1	5.34	1	1	-
	11	pc_BaseTemperature[5]	°Cday	Base temperature during grain filling	0	6	9	9	-
	12	pc_BaseTemperature[6]	°Cday	Base temperature during senescence	9	6	9	9	-
	13	pc_DaylengthRequirement[1]	day	Daylength requirement between sowing and crop emergence	0	-	-	-	-
	14	pc_DaylengthRequirement[2]	day	Daylength requirement between emergence and double ridge	0	12.3	0	0	-
	15	pc_DaylengthRequirement[3]	day	Daylength requirement between double ridge and begin flowering	0	16.67	0	0	-
	16	pc_DaylengthRequirement[4]	day	Daylength requirement between begin flowering and full flowering	0	16.67	0	0	-
	17	pc_DaylengthRequirement[5]	day	Daylength requirement during grain filling	0	-	-	-	-
	18	pc_DaylengthRequirement[6]	day	Daylength requirement during senescence	0	-	-	-	-
	19	pc_BaseDaylength[1]	day	Base daylength between sowing and crop emergence	0	-	-	-	-
	20	pc_BaseDaylength[2]	day	Base daylength between emergence and double ridge	0	1.33	0	0	-
	21	pc_BaseDaylength[3]	day	Base daylength between double ridge and begin flowering	0	1.33	0	0	-
	22	pc_BaseDaylength[4]	day	Base daylength between begin flowering and full flowering	0	1.33	0	0	-
	28	pc_SpecificLeafArea[1]	cm^2/g	Specific leaf area at double ridge	0.002	-	-	-	0.0037
	29	pc_SpecificLeafArea[2]	cm^2/g	Specific leaf area at double ridge	0.0019	-	-	-	0.0015
	30	pc_SpecificLeafArea[3]	cm^2/g	Specific leaf area at double ridge	0.0018	-	-	-	0.0013
	31	pc_SpecificLeafArea[4]	cm^2/g	Specific leaf area at double ridge	0.0017	-	-	-	0.0012
	32	pc_SpecificLeafArea[5]	cm^2/g	Specific leaf area at double ridge	0.0016	-	-	-	0.0012
	33	pc_SpecificLeafArea[6]	cm^2/g	Specific leaf area at double ridge	0.0016	-	-	-	0.0012
OLEARY	1	BASE1	°C	Base temperature for sowing to crop emergence	3	0	-	-	-
	2	BASE4	°C	Base temperature for sowing to anthesis	2	-	-	-	-
	3	BASE5	°C	Base temperature for anthesis to maturity	8	8	-	-	4
	4	DLB4	hour	Base photoperiod for sowing to anthesis	-10	0	-	-	-
	5	EMMDD	°Cday	Thermal time between sowing and crop emergence	100	259	92	438	180
	6	ANTHDL	°Cday	Photothermal time between sowing and anthesis	23700	15012	14158	16677	13800
	7	MATDD	°Cday	Thermal time between anthesis and maturity	465	488	306	677	714
	8	MINTE	kg/ha/mm	Minimum transpiration efficiency	25	-	25	25	58

	9	NTT	°Cday	Period to transfer nitrogen to grain	300	-	-	-	500
	10	GRMAX	mg/day	Maximum grain growth rate	2.8	-	-	-	2.5
	11	GXM	mg	Maximum potential grain dry mass	70	-	-	-	55
	12	PRES	%	Maximum proportion of biomass at anthesis that can be translocated to grain	40	-	-	-	20
	13	SLNOPT	g/m^2	Optimum specific canopy nitrogen	3	-	-	-	2.6
	14	EMOPTT	°C	Optimal temperature for emergence (additional parameter)	-	-	-	-	20
	15	EMMAXT	°C	Maximum temperature for emergence (additional parameter)	-	-	-	-	22
	16	ANOPTT	°C	Optimal temperature for anthesis (additional parameter)	-	-	-	-	20
	17	ANMAXT	°C	Maximum temperature for anthesis (additional parameter)	-	-	-	-	22
	18	MATDD2	°Cday	Thermal time between anthesis and maturity (additional parameter)	-	-	-	-	290
	19	BASE55	°C	Base temperature for anthesis to maturity (additional parameter)	-	-	-	-	15
SALUS	1	LEgg	leaf eq.	Leaf equivalents for grain growth	5.5	6.1	3.7	7.5	6.2
	2	phyll	°Cday	Phyllochron	120	104	79.5	132	102
SIMPLACE	1	PhotoresponseTable	-	Photoperiod reduction factor (for photoperiod < 8 hours/day)	0	0.4	-	-	-
	2	PTTAnthesis	°Cday	Required photo-thermal time (between emergence to anthesis)	289	584.2	725.7	538.3	584.2
	3	TTMaturity	°Cday	Required thermal time between anthesis and maturity	427	425.8	111.3	623.7	425.8
	4	ILAI	-	Initial value of LAI	0.012	-	-	-	0.017
SIRIUS	1	TTBGEB	°Cday	Thermal time between beginning of grain filling and physiological maturity	600	-	400	650	650
	2	TTEGMAT	°Cday	Thermal time between physiological maturity and harvest maturity	150	-	10	140	100
	3	AreaMax	m^2/m^2	Potential maximum leaf surface area	0.004	-	0.005	0.005	-
	4	PHYLL	°Cday	Phyllochron	105	90	105	137	125
	5	AMNLFNO	leaf	Minimum possible leaf number	8	7	6.5	6.5	-
	6	AMXLFNO	leaf	Absolute maximum leaf number	24	18	-	-	-
	7	SLDL	leaf/h daylength	Daylength response in leaf production	0	0.9	0.1	0.1	-
SiriusQuality	1	TTsoem	1/[°Cday]	Thermal time between sowing and crop emergence	190	-	70	390	190
	2	SLDL	leaf/hour daylength	Daylength response of leaf production	0.8	0.79	0.49	4.4	0.79
	3	VAI	1/[°Cd]	Response of vernalization rate to temperature	0	0.004	0	0	0.004
	4	VBBE	1/day	Vernalization rate at 0°C	0	0.02	0	0	0.02
	5	IntermTvern	°C	Intermediate temperature for vernalization to occur	8	15.5	8	8	15.5

	6	MaxTvern	°C	Maximum temperature for vernalization to occur	17	48.5	17	17	48.5
	7	PhyllSSLL	Phyllocron	Potential phyllochronic duration of the senescence period for the leaves produced before floral initiation	3.3	2.8	-	-	-
	8	PhyllSBLL	Phyllocron	Potential phyllochronic duration of the senescence period for the leaves produced after floral initiation	6	2.8	-	-	-
	9	PhyllMBLL	Phyllocron	Potential phyllochronic duration between end of expansion and beginning of senescence for the leaves produced after floral initiation	6	4	-	-	-
STICS	1	stlevamf	°Cday	Thermal time between emergence and end of juvenile phase	245	225	Fixed Anthesis and Maturity	Fixed Anthesis and Maturity	225
	2	stamflax	°Cday	Thermal time between end of juvenile phase and max LAI	390	290	Fixed Anthesis and Maturity	Fixed Anthesis and Maturity	235
	3	stlevdrp	°Cday	Thermal time between emergence and beginning of grain filling	940	563	Fixed Anthesis and Maturity	Fixed Anthesis and Maturity	563
	4	stdrpmat	°Cday	Thermal time between beginning of grain filling and maturity	755	824	Fixed Anthesis and Maturity	Fixed Anthesis and Maturity	824
	5	sensiphot	-	photoperiod sensitivity [0-1] (1 means no sensitivity)	0.8	0.1	Fixed Anthesis and Maturity	Fixed Anthesis and Maturity	0.1
	6	adens	-	Interplant competition parameter	-0.6	-0.6	Fixed Anthesis and Maturity	Fixed Anthesis and Maturity	-0.44
	7	durvieF	-	maximal lifespan of an adult leaf	205	-	Fixed Anthesis and Maturity	Fixed Anthesis and Maturity	175
WHEATGROW	1	IE		Intrinsic earliness	0.91	-	0.71	1.6	0.77
	2	PS		Photoperiod sensitivity	0.00015	-	-	-	-
	3	TS		Thermal sensitivity	0.95	-	0.01	0.98	0.93
	4	BFF		Basic filling factor	0.92	-	0.32	5	0.81
WOFOST	1	TSUM1	°Cday	Thermal time between crop emergence and anthesis	1220	1160	878	1334	-

2	TSUM2	°Cday	Thermal time between anthesis and maturity	770	856	448	1002	-
3	TDWI	kg/ha	Initial total crop DM	210	-	-	-	350
4	FLTB	kg/kg	fraction of above-ground DM to leaves as a function of DVS, at DVS 0.5	0.5	-	-	-	0.6
5	FLTB	kg/kg	Fraction of above-ground DM to leaves as a function of DVS, at DVS 0.646	0.3	-	-	-	0.45
6	FSTB	kg/kg	Fraction of above-ground DM to stems as a function of DVS, at DVS 0.5	0.5	-	-	-	0.4
7	FSTB	kg/kg	Fraction of above-ground DM to stems as a function of DVS, at DVS 0.646	0.7	-	-	-	0.55